phycology

MDPI

Article

Intra-Thallus Variation of Phenolic Compounds and Carbohydrates in *Furcellaria lumbricalis* (Gigartinales, Rhodophyta) from the White Sea (The Arctic Ocean)

Elizaveta Zamyatkina [1], Claudia Wiesner [2,3], Nikolay Yanshin [1], Susan Billig [2] and Elena Tarakhovskaya [1,4,*]

[1] Department of Plant Physiology and Biochemistry, Faculty of Biology, Saint Petersburg State University, Saint Petersburg 199034, Russia; lizatekna@mail.ru (E.Z.); kolya1256@gmail.com (N.Y.)
[2] Institute of Analytical Chemistry, Faculty of Chemistry, Leipzig University, 04103 Leipzig, Germany; birkemeyer@chemie.uni-leipzig.de (C.W.); billig@uni-leipzig.de (S.B.)
[3] German Centre for Integrative Biodiversity Research (iDiv) Halle-Jena-Leipzig, 04103 Leipzig, Germany
[4] Vavilov Institute of General Genetics, Saint Petersburg Branch, Russian Academy of Science, Saint Petersburg 199034, Russia
* Correspondence: elena.tarakhovskaya@gmail.com

Abstract

Furcellaria lumbricalis is an industrially important carrageenophyte. However, beyond the carrageenan characterization, the biochemical composition of this alga remains poorly understood. This study provides the first comprehensive description of the metabolome of *F. lumbricalis* and reveals pronounced biochemical heterogeneity in its thalli by examining the distribution of pigments, phenolic compounds, polysaccharides, and low-molecular-weight metabolites across apical, middle, and basal thallus zones. Understanding the intra-thallus biochemical profiles is necessary for the efficient use of algal feedstock. Untargeted GC-MS analysis of *Furcellaria* extracts revealed a high diversity of phenolic compounds, accounting for 27% of the annotated metabolome. Meristematic apical cells were enriched in organic acids of the TCA cycle, isofloridoside and various phenolic acids, such as caffeic, protocatechuic, and 3,4-dihydroxyphenylpyruvic, indicating active processes of respiration and secondary metabolism presumably conferring chemical defense. Mature cells of the middle zone accumulated carrageenans and heterosides, supporting structural investment and mobile carbon storage. The basal zone, apparently serving both resource storage and stress tolerance functions, featured a relatively high content of mono- and disaccharides, sugar alcohols, floridean starch, *p*-coumaric and 3-phenyllactic acids. Overall, these findings establish a metabolic framework for understanding the functional compartmentalization in red macroalgae and provide a foundation for future studies.

Keywords: *Furcellaria*; red algae; phenolic acids; intra-thallus profiling; metabolomics; caffeic acid; coumaric acid; floridoside; digeneaside

Check for updates

Academic Editor: Adele Cutignano

Received: 18 August 2026
Revised: 15 September 2026
Accepted: 22 September 2026
Published: 24 September 2026

Copyright: © 2026 by the authors. Licensee MDPI, Basel, Switzerland. This article is an open access article distributed under the terms and conditions of the Creative Commons Attribution (CC BY) license.

1. Introduction

Over the past decades, the share of seaweed-based products on the global market has been steadily growing, thus leading to a considerable increase in the annual harvesting of marine macroalgae [1,2]. The most demanded algal species in this regard are those actively used in the production of food and hydrocolloids, such as alginate, agar, and carrageenan. A detailed understanding of the biochemical composition of these algae is crucial for optimizing raw material processing as well as for discovering new natural compounds with valuable properties.

To date, the marine red macroalga *Furcellaria lumbricalis* (Hudson) J.V. Lamouroux 1813 is one of the least studied industrially important carrageenophytes. Along with many other valuable carrageenophytes (*Kappaphycus*, *Eucheuma*, *Chondrus*), *Furcellaria* belongs to the order Gigartinales (Florideophyceae). This is a subtidal alga inhabiting cold waters of the North Atlantic and the Arctic Ocean [3,4]. At present, the largest commercially valuable population is located in the West Estonian Archipelago (Väinameri region, the Kassari Bay), Estonia, where several thousand tons are harvested annually [5,6]. Stock assessments in the Baltic Sea indicate that the average biomass of *F. lumbricalis* ranges from 90 to 691 g m^{-2} in different sub-areas and is subject to considerable annual fluctuations [4,7]. In the Kassari Bay, where *Furcellaria* forms a loose-lying community with *Coccotylus truncatus* (Rhodophyta), the total mixed community biomass has been estimated at 179,000 t. In 2017, it covered an area of 170 km^2, and the mean biomass of *Furcellaria* was reported to be about 600–1000 g m^{-2} [8]. The other substantial populations of this alga are located in the Latvian coastal zone (Pape-Liepaja region, 25,000 t distributed over 139 km^2 in 2003) and near Prince Edward Island in Canada (Gulf of St. Lawrence, 12,300 t distributed over 155 km^2 in 1979) [9,10]. As for the populations in the Arctic Ocean, apparently, no assessments of *Furcellaria* stock have been made yet. According to Shoshina et al. [11], carrageenophyte stocks are limited in the Barents and White Seas, but this statement is not supported by any quantitative data.

Most biochemical studies of *Furcellaria* focus on the specific structural polysaccharides of the alga, in particular its unique carrageenan called furcellaran, which has been industrially manufactured for at least the past 60 years. Although furcellaran manufacture has a smaller market compared to other hydrocolloids, there has been renewed scientific interest in it, particularly in terms of optimizing its production and exploring its unique properties for novel applications [3,12,13]. Furcellaran is a hybrid linear sulphated galactan composed of κ- and β-carrageenan moieties [14]. On average, it constitutes about 20–40% dry weight (DW) of the alga, depending on the ecological form of the thallus (attached/loose-lying) and extraction methods [3,15]. The rheological properties of furcellaran are especially valuable because of its pronounced synergistic interaction with milk proteins. It forms less brittle and smoother gels ideal for the texture improvement of dairy products. Furcellaran is also used as an effective fining agent in the beer and wine industry, as a stabilizer and thickener in personal care products and cosmetics, as a sizing agent for paper and textiles, etc. Also, furcellaran-based films and coatings are reported to have considerable potential in food packaging and targeted drug delivery systems [3,12,14,16].

Surprisingly, beyond studies focused on polysaccharides, to date, little research has been conducted on the detailed biochemical composition of *F. lumbricalis*. Meanwhile, *Furcellaria* accumulates many other valuable molecules, such as the pigment R-phycoerythrin or antioxidant phenolic compounds [17,18]. The available studies provide some general information (mostly for European populations) regarding the total content of pigments, protein, amino acids, carbohydrates, phenolic compounds, lipids, fatty acids and minerals. These data have been summarized in a recent comprehensive review by Kersen et al. [19] and later supplemented by studies by Naseri et al. [20] and Kulikova et al. [21]. However, there is still very little published research based on modern omics approaches, with the exception of single genomic and transcriptomic studies [22,23]. In particular, the detailed metabolome of *F. lumbricalis* mostly remains unstudied. We could find only one study mentioning this species and demonstrating the prevalence of phenolic compounds (presumably, phenolic acids and their derivatives) in the metabolite profile of this alga [24]. Thus, to date, no comprehensive structural identification of low-molecular-weight metabolites of *F. lumbricalis* has been made.

It is now well established that various compounds may be unevenly distributed throughout the thalli of macroalgae. Seaweed can preferentially accumulate metabolites in specific thallus zones or actively allocate them to developing tissues, reproductive organs, or basal structures such as the stipe and holdfast [25,26]. Most investigations considering intra-thallus variation in chemical composition have been carried out on brown algae with large and well-differentiated thalli. Thus, a number of studies have thoroughly examined the distribution of pigments, major minerals, trace metals, phlorotannins and different groups of low-molecular-weight metabolites along the thalli of several fucalean and laminarialean algae, elucidating the source–sink relationships between algal tissues [27–29]. Similar research concerning red algae is much more limited and fragmentary. The intra-thallus distribution of photosynthetic pigments was analyzed only in two species of Bangiales (*Neopyropia yezoensis* and *Porphyra linearis*) [30,31]. Earlier studies addressed the composition and gelling properties of polysaccharides in apices and middle parts of agarophyte *Gracilaria tikvahiae* and carrageenophyte *Kappaphycus alvarezii* [32,33]. Phillips et al. [34] demonstrated the uneven distribution of a specific brominated phenolic compound, lanosol, in the thalli of *Neorhodomela larix* (Rhodophyta). In addition, some works considered the spatial differentiation of nitrogen metabolism, such as the expression of ornithine decarboxylase and polyamine content in *Prionitis imbricata* (Halymeniales) and nitrate and histamine content in *F. lumbricalis* [35–37].

The incomplete understanding of the biochemical composition of *F. lumbricalis* (especially from the Arctic populations) and the lack of data on the distribution of various compounds (including industrially valuable polysaccharides) in its thallus were the key incentives for our research. Thus, the objective of this study was to characterize and compare the biochemical composition of different thallus zones of *F. lumbricalis*, focusing on the compounds with applied relevance. We considered parameters such as pigment, phenolic, and polysaccharide content, as well as low-molecular-weight metabolite profiles.

2. Materials and Methods

2.1. Algal Material

Thalli of *F. lumbricalis* were collected from the typical habitats in the Keret Archipelago (Kandalaksha Bay, White Sea; 66°17′28.76″ N, 33°40′03.46″ E) and directly transported to the laboratory in seawater. The sampling was carried out between late July and mid-August 2023−2025; algal thalli of approximately the same size (12−15 cm) and without visible damage were collected from stones or the rhizoids of *Saccharina latissima* (Phaeophyceae), at a depth of 3−4 m. Samples for biochemical analyses were taken from three thallus zones: (1) basal (lowest part of the thallus, just above the rhizoids), (2) middle, and (3) apical (upper 3 mm) (Figure 1).

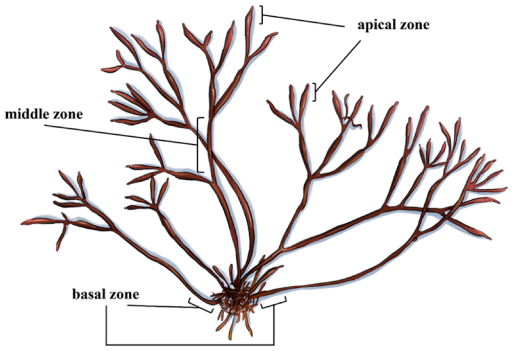


Figure 1. Scheme of the thallus of *Furcellaria lumbricalis* and the zones taken into analysis.

2.2. Dry Weight Determination

For the determination of the dry weight, 100 mg of fresh algal material (FW) was dried at 60 °C to a constant weight.

2.3. Pigment Analysis

The content of photosynthetic pigments in the thalli of *F. lumbricalis* was measured spectrophotometrically. For the analysis of chlorophyll *a* and carotenoids, fragments of algal thalli (10 mg FW) were ground using a mortar and pestle in aqueous acetone (90% for chlorophyll *a* or 80% for total carotenoids) with a small amount of $MgCO_3$. Several rounds of extraction were carried out with additional acetone until the extracts were colorless. The pigment content was calculated based on published equations [38,39] from data obtained with an SF-2000 spectrophotometer (OKB SPECTR LLC, Saint Petersburg, Russia).

For the determination of phycobiliprotein content, fragments of algal thalli (50 mg FW) were homogenized in potassium phosphate buffer (0.1 M, pH 6.8) with a TissueRuptor II homogenizer (QIAGEN, Hilden, Germany) and left soaking at 4 °C overnight. Then the extracts were centrifuged (5000× *g*, 10 min), and the content of phycobilins was determined using an SF-2000 spectrophotometer [40].

2.4. Analysis of Phenolic Compounds

2.4.1. Total Phenolic Content

Samples (20 mg FW) were ground into a fine powder in 1 mL of 70% aqueous acetone and then agitated in the dark for 1 h using a Bio RS-24 mini-rotator (BioSan, Riga, Latvia). Next, the extracts were centrifuged (10,000× *g*, 5 min), the supernatants were transferred into clean microtubes, and 0.5 mL of additional acetone was poured into each residue. After four rounds of extraction, the supernatants were combined, and extract volumes were adjusted to 2.5 mL with 70% acetone. The total phenolic content (TPC) in the extracts was determined by spectrophotometry using the Folin–Ciocalteu assay (modified from [41]). The samples (300 µL) were mixed with 2.4 mL of 5% (*w/v*) sodium carbonate solution and 300 µL of Folin–Ciocalteu reagent. The reaction mixture was incubated at 45 °C for 20 min, and then the absorbance was read at 750 nm (SF-2000). The total content of phenolic compounds was calculated based on a standard curve of gallic acid (Sigma-Aldrich, Steinheim, Germany) and expressed as a percentage of the dry weight.

2.4.2. Content of Flavonoids and Phenolic Acids

The content of flavonoids and phenolic acids was determined according to the published protocol [42]. It should be noted that this method is specific to particular types of phenolic compounds, such as several flavonoids (luteolin, catechin, rutin) and phenolic acids (chlorogenic, caffeic, etc.) possessing a catecholic moiety. We chose this protocol since our test experiments, as well as the literature data, showed that *Furcellaria* is especially rich in these compounds, in particular, phenolic acids. Samples (50 mg FW) were ground in 3 mL of distilled water using a mortar and pestle. Then, the extracts were incubated at 70 °C for 30 min. Following centrifugation (5000× *g*, 10 min), 1 mL of supernatant was mixed with 300 µL of 5% (*w/v*) sodium nitrite, and 5 min later, 500 µL of 2% (*w/v*) aluminum chloride was added. After 6 min, the mixture was neutralized with 500 µL of 1 M sodium hydroxide solution. The samples were left for 10 min at room temperature, centrifuged (5000× *g*, 10 min) and then subjected to spectrophotometric analysis (SF-2000) at 510 nm against the blank, where the aluminum chloride solution had been substituted by water. Catechin (Sigma-Aldrich, Steinheim, Germany) was used as standard for the calibration curve.

2.5. Carbohydrate Analysis

2.5.1. Total Carbohydrate Content

Samples of dried plant material were hydrolyzed in two steps [43]. First, the samples (3 mg DW) were ground into fine powder in 800 µL of 12 M sulfuric acid solution and then left at 30 °C for 1 h. Next, the concentration of sulfuric acid in each sample was adjusted to 1.2 M with distilled water, and the extracts were boiled for 2 h. After cooling, samples were centrifuged (5000× *g*, 10 min). The content of total carbohydrates in the hydrolysates was determined spectrophotometrically using the anthrone reagent [44]. Briefly, 250 µL of the sample (diluted as necessary) was mixed with 2.5 mL of anthrone reagent. The mixture was boiled for 7 min and then immediately cooled in an ice bath. The extinction was measured at 620 nm (SF-2000), and the amount of total carbohydrate was calculated based on a calibration curve with glucose as the standard.

2.5.2. Carrageenan and Floridean Starch Content

The extraction of polysaccharides was carried out using two methods. The first procedure (modified from [45]) leads to the extraction of both carrageenans and floridean starch, while the second procedure [46] allows separation of carrageenans from the other polysaccharide components of algal cells.

Preliminary extraction of polysaccharides. Samples (5 mg DW) were ground in 1 mL of alkaline water (distilled water with the addition of 4 M potassium hydroxide solution, pH 8.8). The extracts were left at room temperature for 1 h and then incubated at 80 °C for 3 h with regular stirring. After centrifugation (10,000× *g*, 5 min), supernatants were transferred into clean microtubes, while the residues were poured into 1 mL of alkaline water and subjected to a second round of extraction (80 °C, 1 h). Then, both supernatants were combined, resulting in the final sample volume being 2 mL.

Procedure 1. The samples were centrifuged (10,000× *g*, 3 min). Next, the supernatant was mixed with 96% ethanol at a ratio of 1:2 and then centrifuged (10,000× *g*, 10 min). The polysaccharide residues were washed four times with ethanol, each time followed by centrifugation and the removal of the supernatant. Finally, the residues were dried at 60 °C and then dissolved in 1 mL of distilled water.

Procedure 2. This method is based on the selective binding and precipitation of carrageenans by cetyltrimethylammonium bromide (CTAB). The extracts (2 mL) were mixed with 250 µL of 2% CTAB solution (in 10% aqueous acetone) and the mixtures were centrifuged (10,000× *g*, 3 min). The precipitates were subsequently washed three times with 96% ethanol saturated with sodium acetate and then three times with pure ethanol. The carrageenan residues were dried at 60 °C and dissolved in 1 mL of distilled water.

Both procedures were followed by the determination of carbohydrate content in the obtained solutions. The content of carbohydrates was measured spectrophotometrically using the anthrone reagent [44]. Absorbance was read at 620 nm (SF-2000). The amount of carbohydrates was calculated based on a standard curve of galactose. The content of floridean starch was calculated as the difference of the values obtained by the two procedures. Accordingly, the method provides an estimate rather than a compound-specific quantification of floridean starch.

2.6. Metabolite Profiling

For the metabolome analysis, samples (50 mg FW) of algal material were quickly ground using a pre-cooled mortar and pestle in 1 mL of cold methanol (−20 °C). A volume of 400 µL of methanol extract was transferred to clean microtubes, vacuum-dried (CentriVap, Labconco, Kansas City, MO, USA) and stored at −80 °C for subsequent analysis. Metabolomic analysis was carried out using gas chromatography–mass spectrometry (GC-

MS) according to the published protocol [47]. Vacuum-dried extracts were subjected to two-step derivatization: in a pyridine solution of methoxyamine hydrochloride (Sigma-Aldrich, Taufkirchen, Germany) and *N*,*O*-bis(trimethylsilyl)-trifluoroacetamide (CS Chromatographie Service GmbH, Langerwehe, Germany). Following derivatization, the samples were transferred to micro-inserts of glass vials and then analyzed using an Agilent 6890 gas chromatograph (0.9 mL/min He flow, splitless mode, injector temperature 280 °C) coupled to an Agilent 5971N quadrupole mass spectrometer (Agilent Technologies, Waldbronn, Germany) with standard electron impact ionization of 70 eV.

In order to calculate the Kovats retention indices (RIs), a mixture of alkanes (C_{10}–C_{32}) in hexane was measured within each sequence [48]. A mixture of 60 authentic standards (amino acids, sugars, sugar alcohols, organic acids, phenolic compounds, etc.) was employed to confirm the identity of expected metabolites.

Deconvolution of chromatographic peaks was achieved using AMDIS 2.65. The retention indices were calculated automatically using an AMDIS calibration file containing the batch retention times of each alkane. The identification of peaks was accomplished using the Golm Metabolome Database (GMD [49]) and NIST14 (Gaithersburg, MD, USA) mass spectral libraries. The integration of the peaks of the corresponding extracted ions ($m/z \pm 0.5$) at specific retention times was performed using the Xcalibur 3.0 (ThermoFisher Scientific Inc., Bremen, Germany) software.

2.7. Data Analysis

The measurements were performed with 4−6 (GC-MS analysis) to 9−12 (other analyses) biological replicates. Each replicate was taken from an individual thallus of *F. lumbricalis*, where samples corresponding to different zones of the thallus were not obtained from the same individuals. Excel 2016 (Microsoft, Redmond, WA, USA) and MetaboAnalyst 6.0 Web application (http://www.metaboanalyst.ca, accessed on 17 June 2026) were used for data processing and normalization procedures as well as for the creation of figures and heatmap construction. The metabolomic data processing involved peak area normalization to the median of all areas within a chromatogram, logarithm transformation (base 10), and range data scaling (mean-centered and divided by the range of each variable). All values are expressed as means and standard deviations. The statistical significance of differences was determined using one-way ANOVA followed by Tukey's HSD post-hoc test, with significance set at $p < 0.05$.

3. Results

3.1. Content of Photosynthetic Pigments in Different Zones of the Algal Thalli

On average, the thalli of *F. lumbricalis* accumulated about 1.46 mg g^{-1} DW of chlorophyll *a* and 0.54 mg g^{-1} DW of total carotenoids, with their amount gradually decreasing from the basal to the apical zone (Figure 2). Thus, apices contained 14 and 35% less chlorophyll and carotenoids, respectively, compared to the basal parts of the thalli. Phycocyanin content showed a reverse trend, increasing by 16% in the apical zone and reaching 4.1 mg g^{-1} DW (Figure 3). The content of phycoerythrin remained rather uniform throughout the thallus and made up about 8 mg g^{-1} DW.

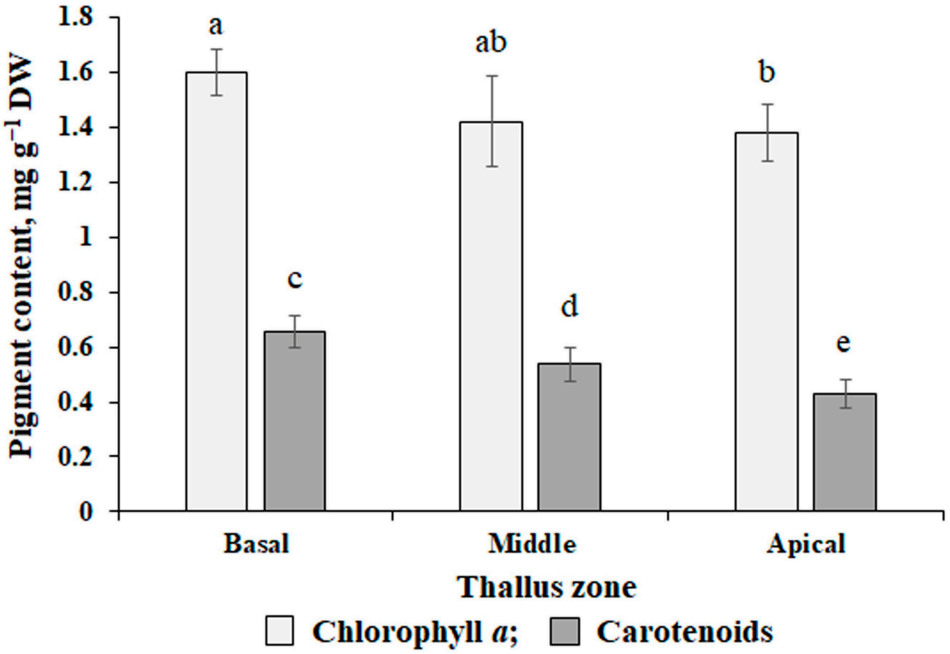


Figure 2. The content of chlorophyll *a* and carotenoids in different zones (basal, middle, apical) of the thalli of *F. lumbricalis*. Means are given with ±SD (n = 6); different letters indicate significant differences ($p < 0.05$, Tukey's HSD post-hoc test).

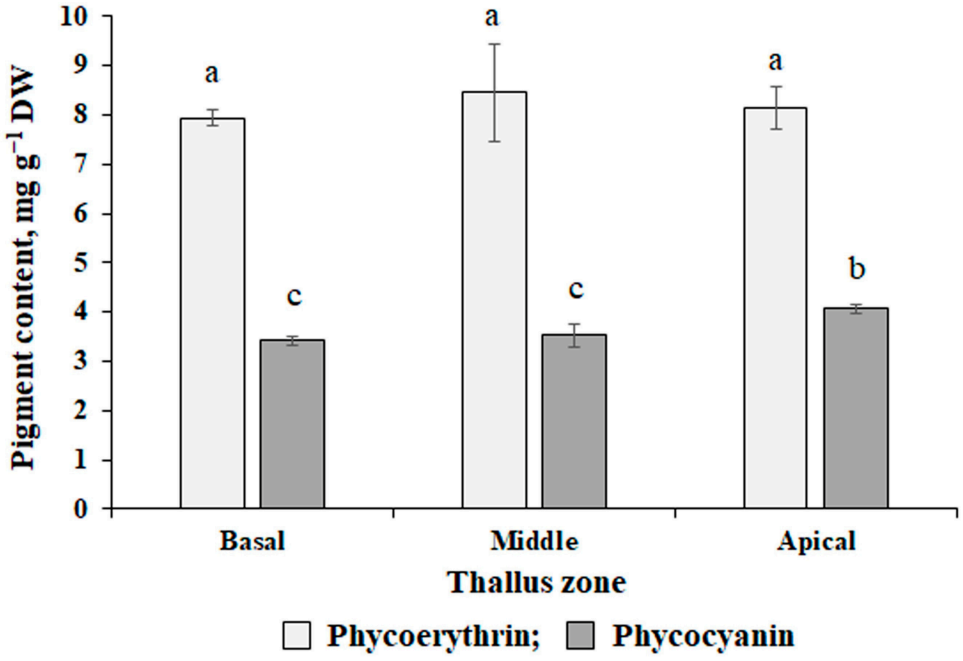


Figure 3. The content of phycobiliproteins in different zones (basal, middle, apical) of the thalli of *F. lumbricalis*. Means are given with ±SD (n = 6); different letters indicate significant differences ($p < 0.05$, Tukey's HSD post-hoc test).

3.2. Total Phenolic Content and Content of Flavonoids and Phenolic Acids in Different Zones of the Algal Thalli

Total phenolic content in the cells of *Furcellaria* thalli was, on average, 2.4% DW, with no statistically significant differences between the three thallus zones (Figure 4a). However, the studied zones clearly differed in the molecular composition of their phenolic compounds: thus, the proportion of flavonoids and phenolic acids was maximal in apices (1.85% DW, which contributes to 76% of TPC) and about two times lower in the rest of the

thallus (Figure 4b). The lowest amount of this phenolic fraction (0.7% DW, 32% of TPC) was found in the cells of the middle zone of *Furcellaria* thalli. It should be noted that the Folin–Ciocalteu and aluminum chloride assays provide complementary colorimetric estimates of extract composition but do not enable identification or compound-specific quantification.

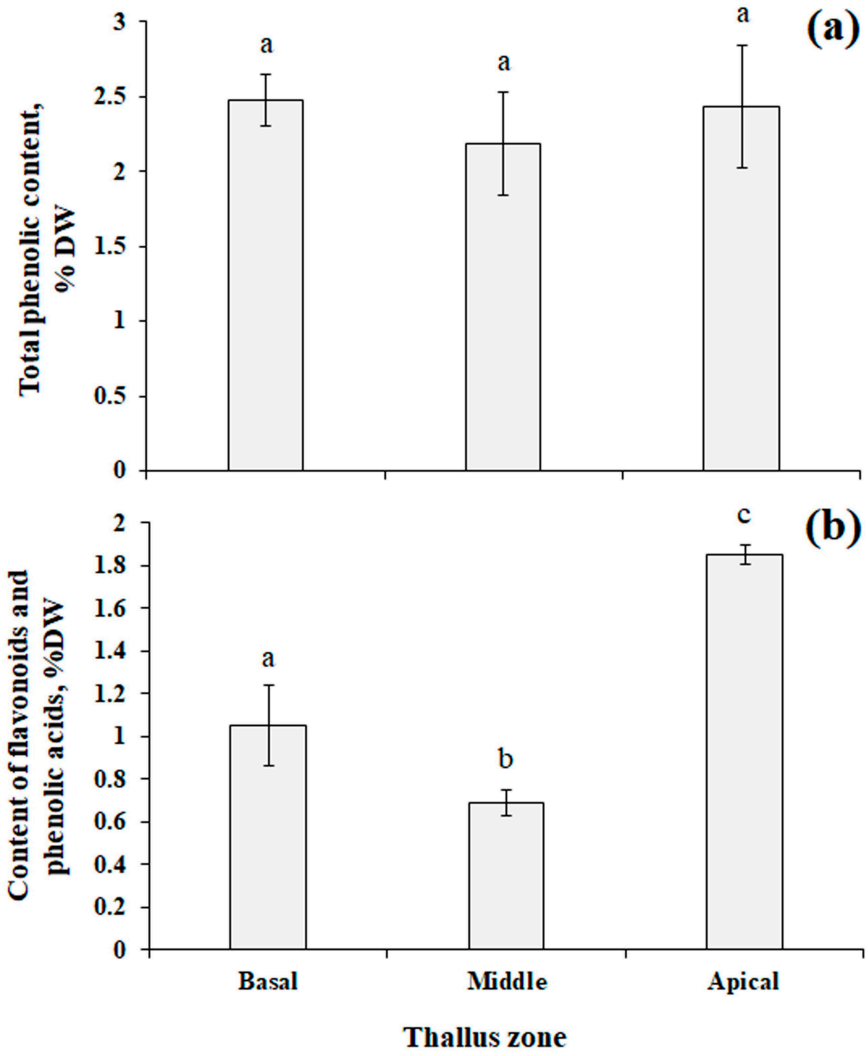


Figure 4. The content of phenolic compounds in different zones (basal, middle, apical) of the thalli of *F. lumbricalis*: (**a**)—total phenolics, (**b**)—flavonoids and phenolic acids. Means are given with ±SD (n = 6–12); different letters indicate significant differences ($p < 0.05$, Tukey's HSD post-hoc test).

3.3. Total Carbohydrate, Carrageenan and Floridean Starch in Different Zones of the Algal Thalli

Carbohydrates were distributed unevenly throughout the thallus of *F. lumbricalis*. The total carbohydrate content was found to be slightly higher in the middle zone of the thallus (up to 49% DW) (Figure 5a). The content of carrageenans amounted to up to 27% DW, with a 44% decline towards the apical zone (Figure 5b). The lowest content of the storage polysaccharide, floridean starch, was characteristic of the middle zone of the *Furcellaria* thallus (2% DW). Approximately 4% DW of this polysaccharide accumulated in other parts of the thallus (Figure 5c).

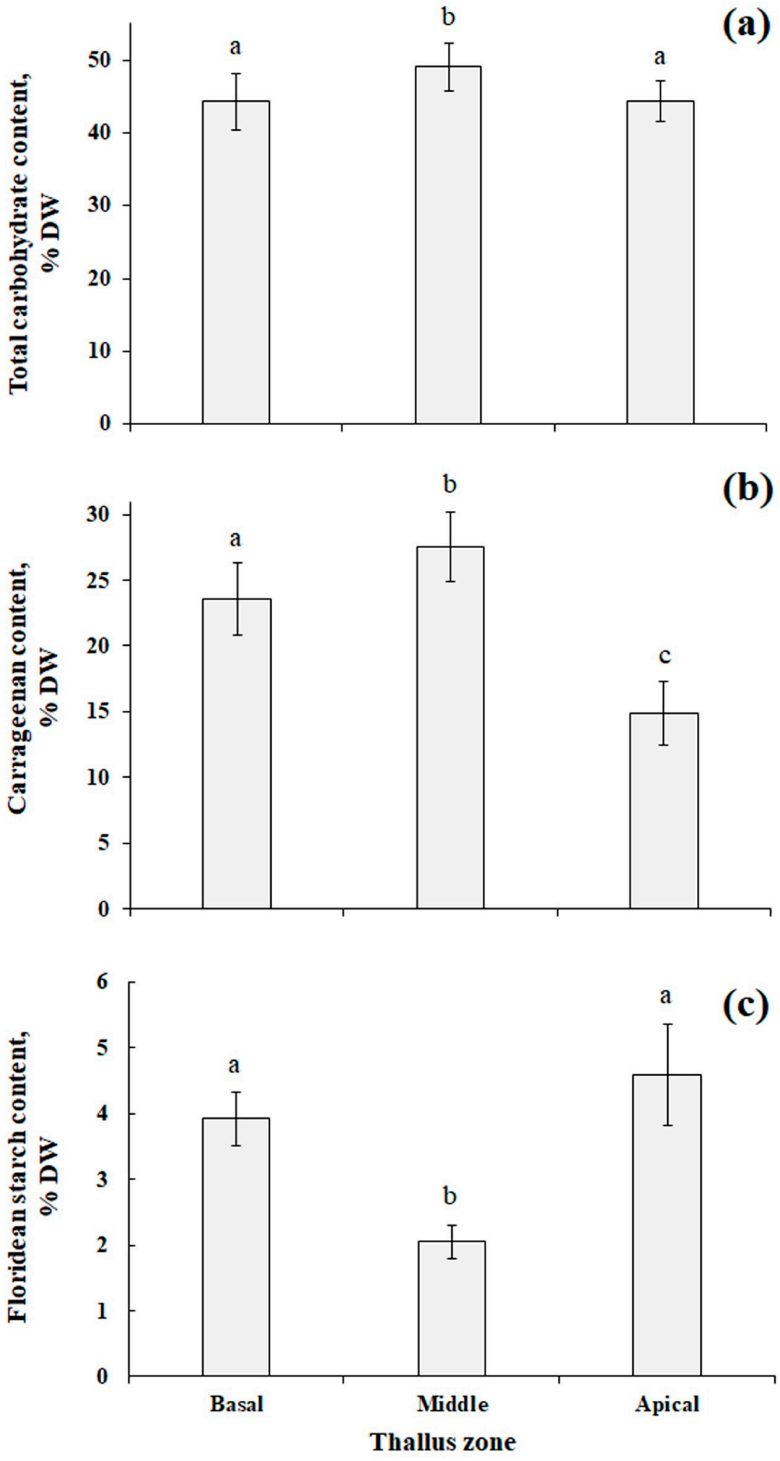


Figure 5. The content of carbohydrates in different zones (basal, middle, apical) of the thalli of *F. lumbricalis*: (**a**)—total carbohydrates, (**b**)—carrageenans, (**c**)—floridean starch. Means are given with ±SD (n = 9–12); different letters indicate significant differences ($p < 0.05$, Tukey's HSD post-hoc test).

3.4. Low-Molecular-Weight Metabolite Profiles in Different Zones of the Algal Thalli

GC-MS-based profiling led to the detection of 211 metabolites in the *Furcellaria* thalli, about 80% of which were either identified or structurally annotated to specific chemical classes (see Table S1 for details). The metabolite profile comprised 62 carbohydrates, 13 organic acids, 20 amino acids (including the non-proteinogenic amino acids β-alanine, γ-aminobutyric acid, and ornithine along with amino acid derivatives), 17 lipid-related metabolites, and 45 phenolic compounds. The metabolome of *F. lumbricalis* was dominated

by specific glycosides (floridoside, isofloridoside, digeneaside), phenolic acids (caffeic acid, *p*-coumaric acid), as well as several sugar alcohols (glycerol, mannitol) and organic acids (citric acid). To elucidate the major trends in the variation of low-molecular-weight metabolite profiles across different thallus zones, the dataset was subjected to partial least squares discriminant analysis (PLS-DA, Figure 6). The results of cross-validation and permutation tests are presented in Figure S1. The heatmap (Figure 7) displays the relative abundances of the identified metabolites with the highest absolute loading values obtained from PLS-DA.

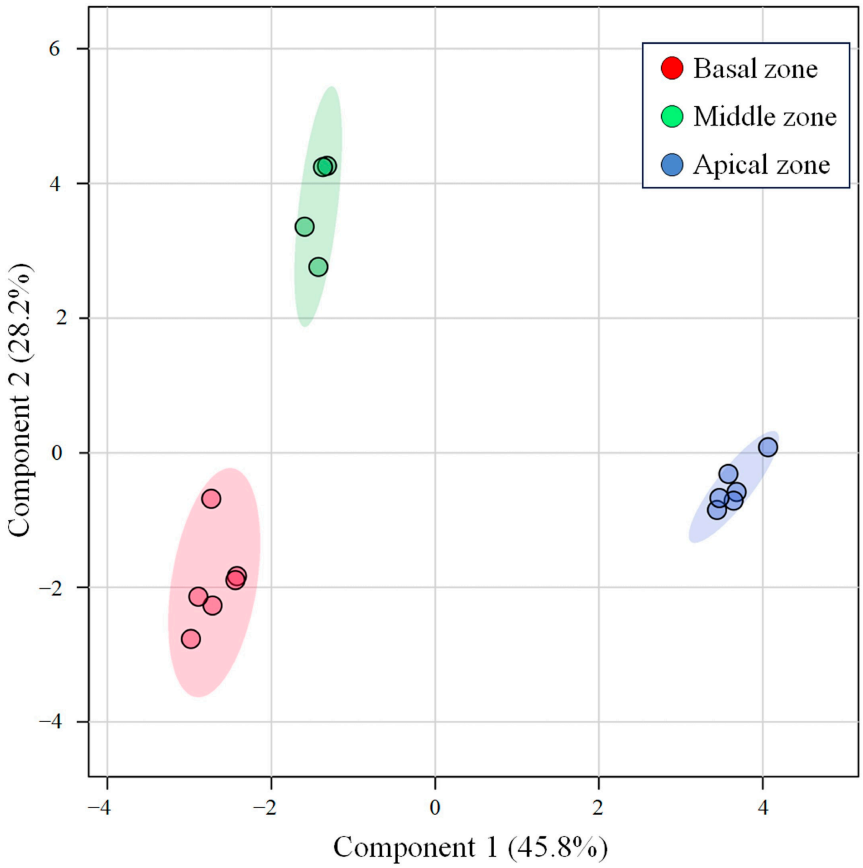


Figure 6. Sample scores for the first two components derived from PLS-DA of the relative metabolite concentrations in different thallus zones (basal, middle, and apical) of *F. lumbricalis*.

PLS-DA revealed clear clustering of samples from different thallus zones along the first component, which accounted for approximately 46% of the total variance in the dataset (Figure 6). The greatest contribution to the first component was made by sugars (sucrose, trehalose, mannose), sugar alcohols (mannitol, glycerol, sorbitol), organic acids (citric, isocitric, α-ketoglutaric), and glycosides (isofloridoside, digeneaside). The second component, explaining approximately 28% of the variance, revealed some biochemical similarity between samples from the apical and basal thallus zones. The main loadings for this component were represented by phenolic acids (*p*-coumaric, caffeic, 4-hydroxyphenylpyruvic), sugar alcohols (erythritol, *myo*-inositol), amino acids (glutamic acid, valine, β-alanine), and several monosaccharides (fructose, glucose, galactose).

The apical zone of *Furcellaria* thalli was characterized by elevated levels of TCA-cycle organic acids (citric, isocitric, cis-aconitic, etc.), the sugar alcohol myo-inositol, and the glycoside isofloridoside (Figure 7). Cells in this zone also showed the accumulation of specific amino acids and phenolic acids (protocatechuic, caffeic). In addition, cells of

the apical zone contained high amounts of hydroxylated derivatives of phenyllactic and phenylpyruvic acids.

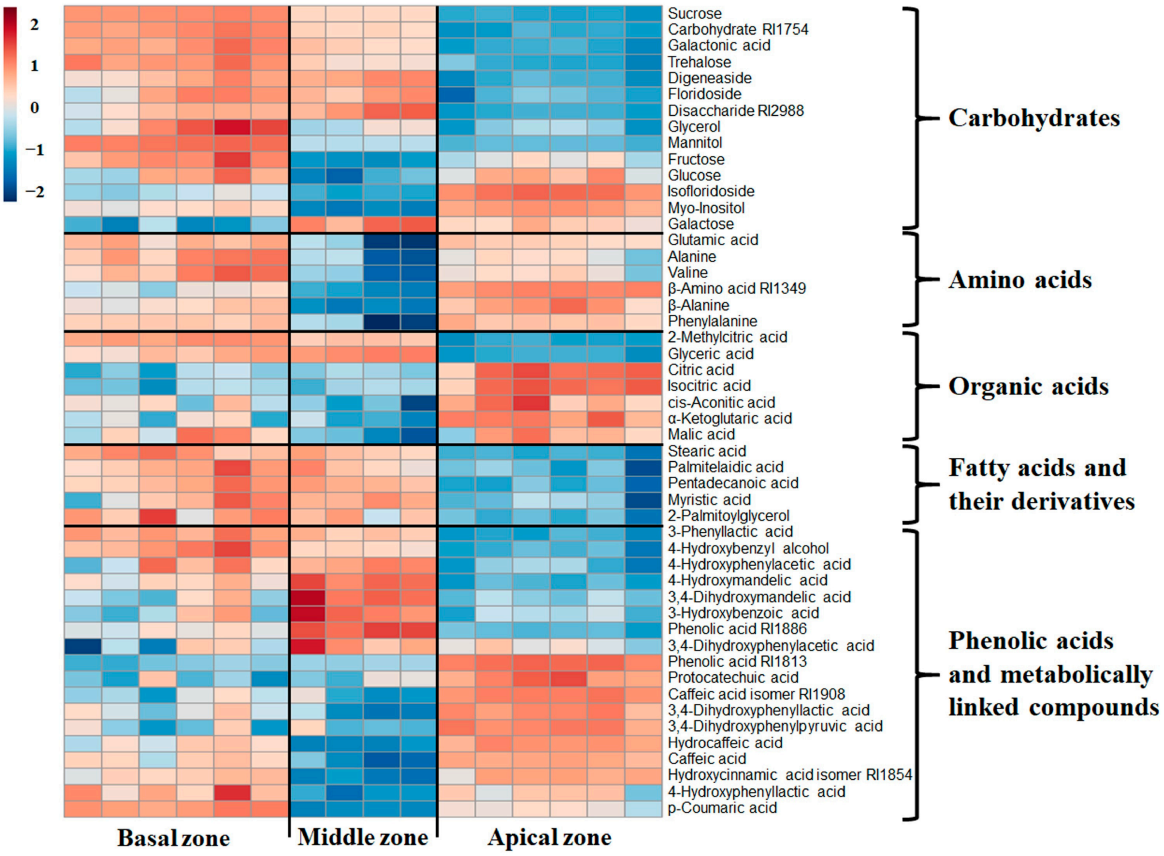


Figure 7. A heatmap of key metabolites with significantly ($p < 0.05$, Tukey's HSD test, FDR correction) different relative abundances in the basal, middle, and apical zones of *F. lumbricalis* thalli. Values are presented on a $\log_{10}$ scale. The confidence level of the tentative identifications for the metabolites included in this figure is given in Table S1.

The middle zone of the *Furcellaria* thalli was distinguished by reduced levels of amino acids (glutamic acid, alanine, valine, *β*-amino acids) and organic acids of the TCA cycle (Figure 7). In contrast, cells in this zone actively produced storage glycosides (digeneaside, floridoside) and galactose, along with fatty acids (stearic, myristic, pentadecanoic, etc.). The profile of dominant phenolic acids in the middle zone differed markedly from that in the apices, being dominated by 4-hydroxyphenylacetic acid, 4-hydroxymandelic acid, their derivatives, and 3-hydroxybenzoic acid.

Cells of the basal thallus zone accumulated a diverse array of carbohydrates (glycosides, sugar alcohols, disaccharides), as well as amino acids (glutamic acid, alanine, valine) and fatty acids (Figure 7). The galactose level in this zone was notably lower. Among the phenolic compounds, *p*-coumaric acid, 3-phenyllactic acid, and gastrodigenin (4-hydroxybenzyl alcohol) predominated in the thallus base.

4. Discussion

4.1. General Biochemical Composition of F. lumbricalis

Our results regarding the general biochemical composition of *F. lumbricalis* largely corroborate earlier findings, with some exceptions related to pigment content. Thus, while chlorophyll *a* content (~1.5 mg g^{-1} DW) was in full agreement with the literature data, the amount of total carotenoids was found to be three times higher compared to previously

published values (Figure 2) [50,51]. This may be related to seasonal or geographical variation. Considerable seasonal changes in photosynthetic pigment levels, including carotenoids, have been documented for several red algal species [52,53]. The content of phycoerythrin and phycocyanin (~8 and 4 mg g^{-1} DW, respectively) (Figure 3) was in accordance with previous data for the White Sea *Furcellaria* population, but exceeded the values obtained for the algae collected in the Baltic Sea [51,54,55]. In addition to seasonal and geographical factors, these differences may also be explained by the extraction methods employed, in particular for phycobiliproteins, as these pigments are sometimes difficult to extract [55]. The values for total phenolic and carbohydrate content, as well as carrageenan and floridean starch levels, obtained in our study (Figures 4 and 5) are within the ranges reported in earlier works [3,15,17,21,51,56–58]. The floridean starch and TPC data should be treated as approximate estimates rather than definitive values, given the constraints of the methods employed.

4.2. General Considerations for Metabolite Profiling

To our knowledge, this study provides the first detailed characterization of the low-molecular-weight metabolite profiles in the cells of *F. lumbricalis*. The most striking feature revealed by GC-MS analysis is the unusually high diversity and abundances of phenolic metabolites, which account for 27% of the total annotated metabolome of this alga (Table S1). This is consistent with our data (Figure 4a) and earlier studies showing that, compared with other gigartinalean algae, *F. lumbricalis* is characterized by a relatively high level of phenolic compounds [17]. Reported TPC in representatives of Gigartinales vary in the range of 0.02–1% DW [59,60]. Among red algae, TPC values comparable to those of *F. lumbricalis* were found only in a few species belonging to Rhodomelaceae (Ceramiales) and accumulating various bromophenols, such as lanosol, rhodomelol, etc. [59,61,62]. However, the phenolic profile of *F. lumbricalis* was found to be quite different from those of ceramialean species: it was dominated by various types of phenolic acids (hydroxybenzoic, phenylacetic, phenylpropanoids, etc.) (Figure 7, Table S1), with caffeic and *p*-coumaric acids being the major phenolic metabolites. Although the presence of phenolic metabolites in red algae has been studied quite thoroughly in general, detailed studies have addressed almost exclusively halogenated compounds such as bromophenols from the order Ceramiales [62–64], while phenolic acids were mentioned only in single works. Thus, protocatechuic, caffeic and *p*-coumaric acids, as well as metabolically linked benzoic acid, have been found in several species of the order Gigartinales (*Chondrus crispus*, *Mastocarpus stellatus*, *Gigartina pistillata*) [60], and structurally related sulfated phenylpropanoids have been identified in another gigartinalean alga, *Tichocarpus crinitus* [65]. A rich pattern of phenolic acids in the cells of *F. lumbricalis* suggests a high activity of the shikimate pathway, with various branches of this route making unequal contributions in different thallus zones (Figure 8).

Another group of low-molecular-weight metabolites, abundantly present in cells of *F. lumbricalis* and accounting for ~30% of the analyzed metabolome, includes various carbohydrates, among which specific glycosides (heterosides: floridoside, isofloridoside, digeneaside) and sugar alcohols (glycerol, mannitol) predominate (Table S1). Floridoside and its isomers are widely distributed in red algae, reported to be present in at least 164 species of 85 genera, including *F. lumbricalis* [66,67]. However, to our knowledge, this study is the first documentation of digeneaside occurrence in *F. lumbricalis*. This heteroside was initially thought to be a distinctive storage metabolite specific for representatives of the order Ceramiales, but subsequent research demonstrated that many representatives of other orders (including Gigartinales) are also capable of its synthesis [68,69]. In a comparative study by Karsten et al. [69], six out of seven species of the Gigartinales were shown to accumulate both floridoside and digeneaside, which is consistent with our results. Thus,

the co-occurrence of both these heterosides may be a common chemotaxonomic feature within this order. In red algae, floridoside (and its isomers) and digeneaside are the main products of photosynthesis, serving as soluble storage compounds and osmolytes [66]. The accumulation of glycerol in *Furcellaria* cells most likely reflects its involvement in the metabolism of heterosides (Figure 9). In addition, this relatively inert compound can also contribute to osmoregulation [70].

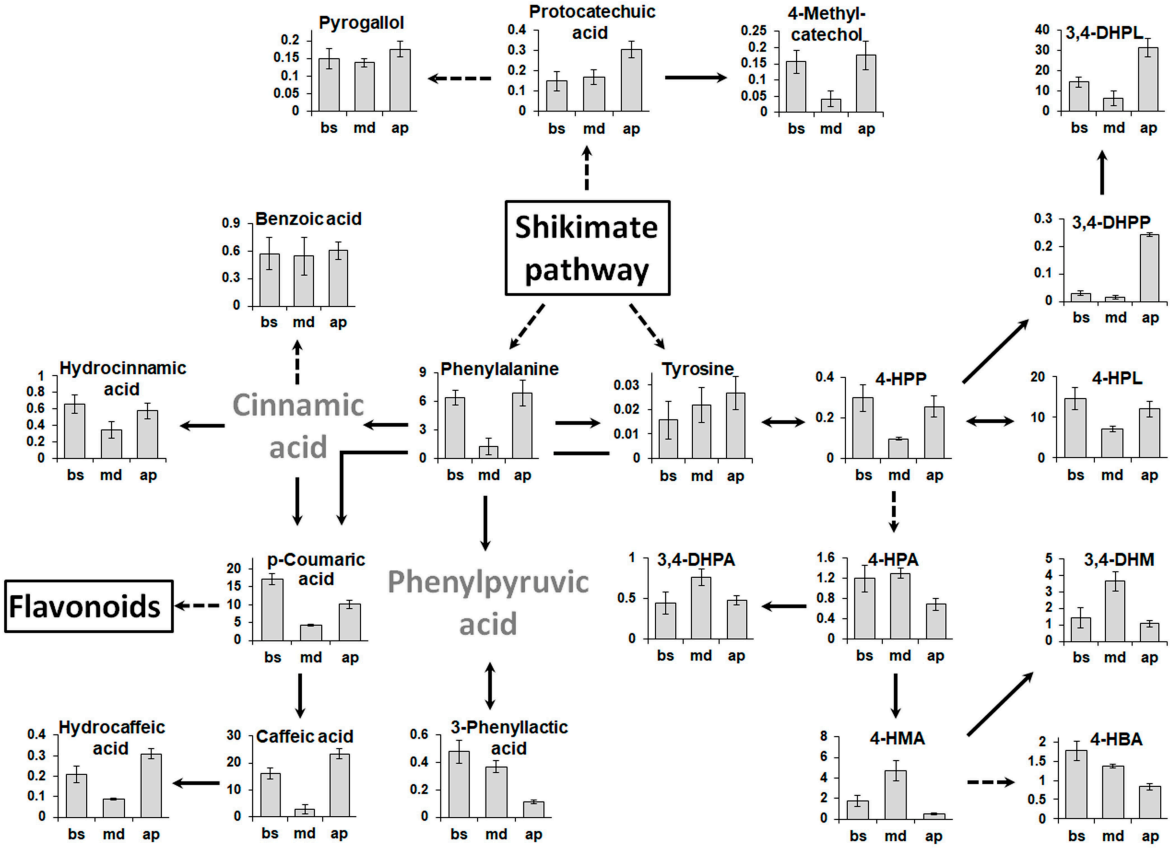


Figure 8. Scheme of the metabolic pathways of phenolic acids in different thallus zones of *F. lumbricalis*. Direct reactions are presented as straight lines and reactions involving several steps are presented as dashed lines. Relative metabolite content is given in arbitrary units, which are normalized peak areas of extracted ion chromatograms. Metabolites that were not determined are labeled in grey. bs—basal zone, md—middle zone, ap—apical zone, 3,4-DHM—3,4-dihydroxymandelic acid, 3,4-DHPA—3,4-dihydroxyphenylacetic acid, 3,4-DHPL—3,4-dihydroxyphenyllactic acid, 3,4-DHPP—3,4-dihydroxyphenylpyruvic acid, 4-HBA—4-hydroxybenzyl alcohol, 4-HMA—4-hydroxymandelic acid, 4-HPA—4-hydroxyphenylacetic acid, 4-HPL—4-hydroxyphenyllactic acid, 4-HPP—4-hydroxyphenylpyruvic acid. Bars represent the means ± SD. The confidence level of the tentative identifications for the metabolites included in this scheme is given in Table S1.

The isolation of another sugar alcohol, mannitol, from *F. lumbricalis* was originally reported by Lindberg [67]. However, a subsequent reinvestigation by Kremer [71] refuted this finding, attributing it either to contamination by epiphytic diatoms or to misidentification. Mannitol had long been considered rare among red algae, with confirmed findings limited to several ceramialean species (e.g., *Caloglossa* sp.) and representatives of the Rhodellophyceae [72,73]. Our detection of mannitol in *F. lumbricalis* corroborates the initial results of Lindberg [67], who also emphasized the considerable abundance of this compound in the samples, making contamination an improbable explanation. This result is consistent with recent data by Hamid et al. [74], who examined five red algal species of different orders and showed that the Gigartinales alga, *Neodilsea yendoana*, featured the

highest content of mannitol. Thus, our finding extends the known distribution of this polyol within Rhodophyta.

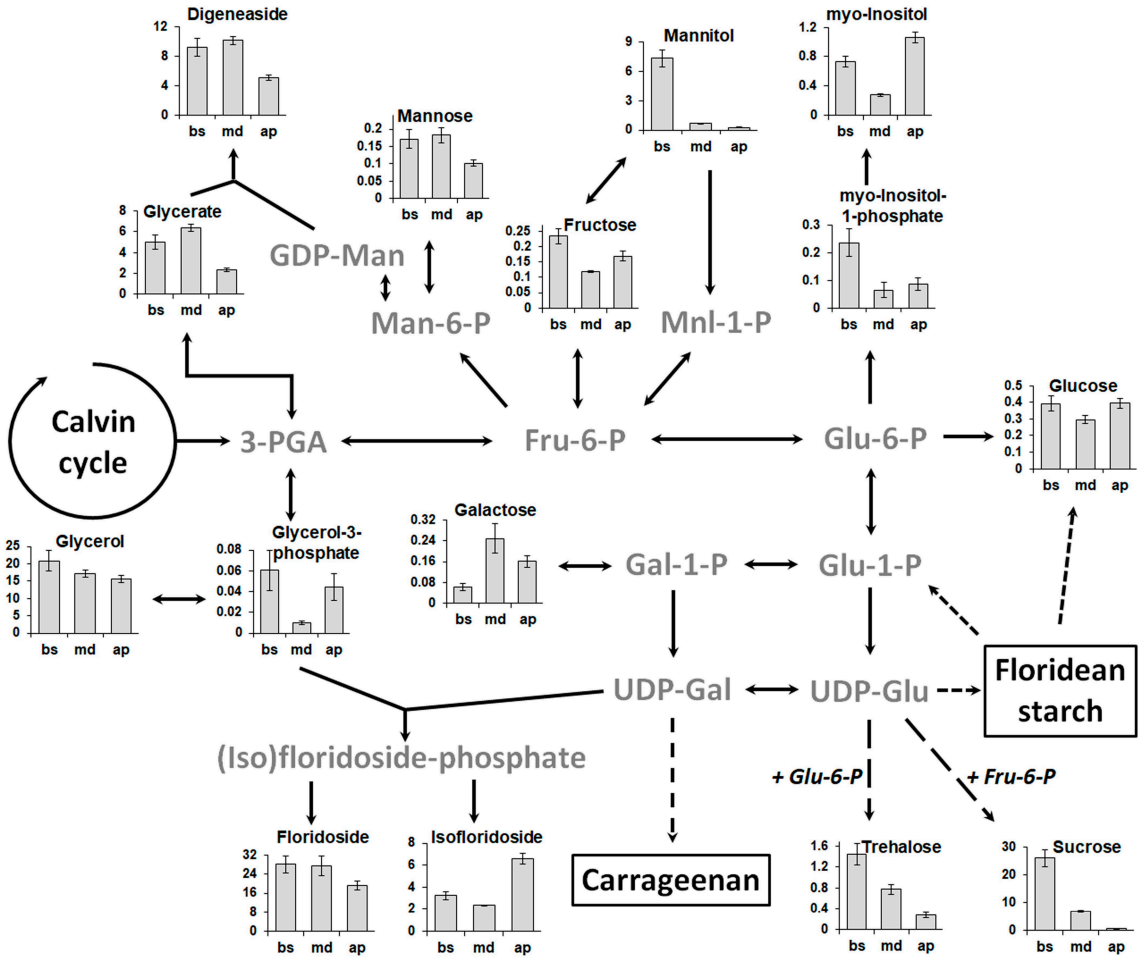


Figure 9. Scheme of the central carbon metabolism and polysaccharide biosynthetic pathways in different thallus zones of *F. lumbricalis*. Direct reactions are presented as straight lines and reactions involving several steps are presented as dashed lines. Relative metabolite content is given in arbitrary units, which are normalized peak areas of extracted ion chromatograms. Metabolites that were not determined are labeled in grey. bs—basal zone, md—middle zone, ap—apical zone, GDP-Man—GDP-mannose, Man-6-P—mannose-6-phosphate, Mnl-1-P—mannitol-1-phosphate, 3-PGA—3-phosphoglyceric aldehyde, Fru-6-P—fructose-6-phosphate, Glu-6-P—glucose-6-phosphate, Glu-1-P—glucose-1-phosphate, Gal-1-P—galactose-1-phosphate, UDP-Gal—UDP-galactose, UDP-Glu—UDP-glucose. Bars represent the means ± SD. The confidence level of the tentative identifications for the metabolites included in this scheme is given in Table S1.

Among other carbohydrates present in cells of *Furcellaria*, the disaccharide trehalose deserves special mention. While Karsten et al. [69] did not detect trehalose in any investigated members of the Gigartinales, we successfully identified this compound in *F. lumbricalis*. This result accords with other reports of trehalose in several Gigartinales species, such as *Cystoclonium purpureum* and *Euthora cristata* [51]. Therefore, this compound may be more widespread among Rhodophyta than previously thought.

One more interesting finding in the metabolome of *F. lumbricalis* is a compound tentatively annotated as *β*-amino acid RI1349 (Table S1). According to chromatographic data, this is a relatively abundant metabolite, specifically accumulating in the apical zone of the thallus, which implies its physiological significance. Figure S2 provides spectral information supporting the annotation of this compound as well as putative structures.

The structure may be related to *N*-alkylated *β*-alanine or hydroxy-*β*-proline and might represent one of its derivatives. Notably, intra-thallus distribution of *β*-amino acid RI1349, in general, correlates with that of *β*-alanine (r = 0.82). Overall, among seaweeds, red algae, in particular representatives of the order Gigartinales, are considered to be the principal producers of *β*-alanine and its derivatives, such as *β*-alanine-containing dipeptides (carnosine, anserine), so the possible presence of one more compound of this type does not seem counterintuitive [75,76]. *β*-amino acid derivatives are increasingly recognized as natural algal products, appearing as dipeptides in brown, green and red algae, as N-methylated neurotoxins (*β*-*N*-methylamino-L-alanine) in diatoms, dinoflagellates, and Cyanobacteria, and as betaines (*β*-alanine betaine, hydroxy-*β*-proline betaine) in green and brown macrophytes [77–80]. However, at present, the definite identity of *β*-amino acid RI1349 remains uncertain and further studies are required for reliable identification of this interesting compound.

4.3. Intra-Thallus Biochemical Heterogeneity

For the first time, the results of our study indicate pronounced biochemical heterogeneity of *Furcellaria* thalli. The mechanisms underlying this phenomenon remain uncertain, as red algae are much less studied in this aspect than brown and green algae. The differences in the biochemical composition of the three thallus zones could be simply attributed to the processes of cell differentiation and tissue aging, resulting in the inherent morphological and physiological diversity of the cells throughout the thallus (e.g., [32,33]). So far, however, to our knowledge, the morphological and anatomical characteristics of the cells from different thallus zones of *Furcellaria* have not been examined in detail. Another possible explanation would be the occurrence of long-distance transport and source–sink relationships between the cells differing in their position in the thallus. The existence of such mechanisms in Rhodophyta remains a matter of debate, despite well-authenticated evidence for the translocation of substances along the thalli of several species [81–85]. Indeed, it cannot be ruled out that both proposed mechanisms are involved here, so that the net content of certain compounds in the cells of the algae is dependent on the joint effect of the cell position, photosynthetic capacities, and physiological status (division frequency, level of differentiation, etc.).

4.3.1. Apical Zone of the Thallus

Thalli of *F. lumbricalis* are characterized by apical growth, so apices (Figure 1) contain actively dividing meristematic cells [3]. Obviously, this is the main factor determining the specific biochemical composition of this thallus zone. Our study showed that the content of photosynthetic pigments, chlorophyll *a* and carotenoids, gradually decreased from the base towards the apices of the *Furcellaria* thalli (Figure 2). This finding supports the earlier observation of Adamkiewicz-Chojnacka [86], who reported the tips of the branches of this alga to seem considerably lighter, suggesting lower pigment content. Studies on other red and brown algae have demonstrated that meristematic regions of the thalli typically have the lowest pigment content [27,31], which is consistent with our data. Interestingly, the intra-thallus distribution of phycobilins did not coincide with that of other photosynthetic pigments: instead, phycocyanin accumulated in the apices of *Furcellaria* thalli (Figure 3). This may reflect an additional physiological role of phycobilins: apart from contributing to the light-harvesting process during photosynthesis, these nitrogen-rich molecules also serve as an intracellular nitrogen reserve [87]. Thus, we suggest that the apical zone of the *Furcellaria* thallus has an underdeveloped photosynthetic apparatus (which explains the lower content of chlorophyll and carotenoids) but actively synthesizes phycobilins for nitrogen storage to support the high metabolic demand of dividing meristematic

cells [30,36]. Accordingly, the highest nitrate content was earlier reported for *Furcellaria* apices [36], and metabolite profiling showed that, compared to the mid-thallus, apices had a relatively high content of several free amino acids (in particular, glutamic acid), indicating active nitrogen metabolism in this zone (Figure 7). Taking into account the relatively low content of these compounds in the middle zone of the thallus, we may suppose that acropetal transport is involved in free amino acid distribution. Although we did not assess metabolite translocation in this study, long-distance transport of amino acids towards the actively growing regions has been shown earlier in red [84] and brown [28,88,89] algae. A relatively high content of organic acids of the TCA cycle (citric, isocitric, α-ketoglutaric acid, etc.) and β-alanine (a component and a metabolic precursor of pantothenic acid) suggests elevated respiratory activity in the apices of *Furcellaria*, which is also typical for meristematic cells of both macroalgae and vascular plants [28,90,91]. However, direct measurements of metabolite translocation and respiratory activity in *Furcellaria* thalli are required to experimentally validate these hypotheses.

Analysis of carbohydrate profiles in the apical zone of *Furcellaria* thallus showed that, compared to the middle zone, apices feature a reduced content of major structural polysaccharides (carrageenans), but relatively high amounts of storage polysaccharide (floridean starch) and several low-molecular-weight carbohydrates (isofloridoside, glucose, fructose, myo-inositol) (Figures 5, 7 and 9). This is logical for meristematic and not fully differentiated cells with reduced photosynthetic activity: such cells have relatively thin walls capable of stretching during cell growth and, therefore, preferably invest assimilated carbon not in metabolically inert cell wall constituents (such as carrageenans), but in more labile compounds necessary for maintaining active metabolism. Since the apical zone may function as a sink for photoassimilates in the case of long-distance transport, organic carbon is stored there in an insoluble form (granules of floridean starch). Adjusting the principal direction of the carbon flux into storage or structural carbohydrate pools in response to current physiological needs was earlier shown in red algae [92]. Similar trends in the intra-thallus distribution of structural and reserve polysaccharides were also reported for several red algal species. Thus, an elevated level of floridean starch was found in the apices of *Kappaphycus alvarezii*, compared to the middle zone of the thallus [33]. Craigie and Wen [32] obtained half the agar yield from young tissues of apical thallus segments, compared to mature segments in *Gracilaria tikvahiae*. Interestingly, these authors also showed that the age of the cells (and consequently, their position in the thalli) affects the biochemical composition of agar (sulfate content, 3,6-anhydrogalactose content, number of methylated galactose residues) and the quality of the gels: optimal gel-forming properties were found for agar extracted from the apices of the *Gracilaria* thallus [32]. This opens new avenues for detailed investigation of carrageenans in *F. lumbricalis*, as similar differences in carrageenan composition and quality may be expected in various thallus zones of this carrageenophyte.

An interesting result is the difference in the floridoside/isofloridoside ratio between the apical and middle zones of *Furcellaria* thalli: isofloridoside specifically accumulates in the apices of the alga, while this zone contains the lowest level of floridoside (Figures 7 and 9). As early as 1968, it was suggested that, despite their structural similarity, these two metabolites are not equivalent and interchangeable [93]. Furthermore, later, it was shown that their metabolic precursors, floridoside and isofloridoside phosphates, are synthesized by different enzymes [66]. Although the physiological significance of the differential accumulation of galactosylglycerol isomers in red algae remains largely unclear, some evidence suggests that while floridoside primarily serves as a storage compound, isofloridoside rather contributes to stress tolerance by acting as an osmolyte [66]. This is in line with the hypothesis of Raven et al. [94] that a single compound cannot effectively function as both a respiratory substrate and an osmolyte unless complemented by another

compatible solute. In *F. lumbricalis*, an intra-thallus profile similar to that of isofloridoside was also shown for myo-inositol (Figure 9). Since these two carbohydrates are not directly metabolically linked, their co-accumulation in the apices most likely relates to their common function: both compounds can protect developing tissues from osmotic stress [95]. The relatively high content of these compounds in the apical zone, compared to the mid-thallus (Figure 9), implies a possible source–sink relationship, as was recently demonstrated for *Pyropia haitanensis* [96].

Our data showed that, despite similar TPC, the examined zones of *Furcellaria* thalli have qualitatively different profiles of phenolic metabolites (Figures 4 and 7). The apical zone is distinguished by the highest content of the phenolic fraction, which contains flavonoids and phenolic acids bearing the catecholic moiety (Figure 4b). Since GC-MS analysis revealed a high prevalence of phenolic acids in the metabolome of *Furcellaria* (Table S1), it is most likely that these compounds, rather than flavonoids, are the largest contributors to this phenolic fraction. Relatively high levels of phenolic metabolites associated with different branches of the shikimate pathway and phenylalanine/tyrosine metabolism (e.g., protocatechuic acid, cinnamic and 4-hydroxyphenylpyruvic acid derivatives, Figure 8) suggest generally increased intensity of phenolic acid biosynthesis in *Furcellaria* apices. The notable exception here is 4-hydroxyphenylacetic acid and its derivatives (mono- and dihydroxymandelic acids, etc.), which mainly accumulate in the middle and/or basal zones of *Furcellaria* thalli. Relatively low abundance of 3-phenyllactic acid, a product of phenylalanine catabolism, may result from the enhanced consumption of phenylalanine to produce various phenolic acids (Figure 8).

Specific accumulation of different types of phenolic acids in *Furcellaria* apices is most likely associated with the protective functions of these compounds. Both terrestrial plants and seaweeds were shown to concentrate defensive metabolites in younger tissues, with apically growing species having the highest levels in the meristematic tips [26]. Thus, protocatechuic acid (and its derivatives, such as pyrogallol) exhibits antioxidant, allelopathic and antibacterial properties [97]. Caffeic acid, one of the dominant phenolic metabolites in *Furcellaria* cells, is known as a potent stress-modulating compound with antioxidant and antimicrobial activities [98–100]. In addition to acting as antioxidants, dihydroxyl derivatives of phenyllactic and phenylpyruvic acids, particularly abundant in the apices of *F. lumbricalis*, are also metabolic precursors in the biosynthesis of other bioactive phenolic acids with larger molecules, such as rosmarinic acid [101]. This compound has been identified in representatives of several orders of red algae [102]. Besides phenolic metabolites, cells of the apical zone of *Furcellaria* thalli accumulated β-alanine (Figure 7), another compound known as a protective plant and algal metabolite [75,103]. The putative derivative of this non-proteinogenic amino acid, β-amino acid RI1349 (Figure S2, Table S1), might have similar properties. One more physiological reason for maintaining a relatively high content of several phenolic acids in the meristematic zone of the thallus may be the growth-stimulating activity of these compounds. Thus, exogenous caffeic acid, protocatechuic acid (along with the metabolically related compound, 4-methylcatechol), and 4-hydroxyphenylpyruvic acid have previously been shown to effectively stimulate growth of the red algae *Stylonema alsidii* and *Neopyropia tenera* [104,105].

4.3.2. Middle Zone of the Thallus

Analysis of the middle zone of the *Furcellaria* thallus (Figure 1) provides a "snapshot" of metabolic processes typical for mature, fully differentiated cells, which make up most of the thallus volume. Anatomically, this zone is heterogeneous: it contains peripheral layers of relatively small, highly pigmented, and actively photosynthesizing cells and the inner core cells with lower pigmentation, which are relatively large, have an elongated

tubular shape, and are tightly connected to each other [86]. In the physiological context, assuming the contribution of long-distance transport to resource allocation, we hypothesize that the middle part of the thallus may act as a source zone supplying the entire alga with photosynthetic products. Further research is needed to test this hypothesis.

Our results indicated that the mid-thallus accumulates the highest amounts of both total carbohydrates and carrageenans, structural polysaccharides of the *Furcellaria* cell walls (Figure 5a,b). This is consistent with metabolomics data showing a specific accumulation of galactose in these cells (Figures 7 and 9), as this monosaccharide is a structural unit and metabolic precursor of carrageenans. With respect to storage carbohydrates, the cells of the mid-thallus are relatively rich in the predominant low-molecular-weight metabolites, floridoside and digeneaside (Figure 9), but contain half as much floridean starch as the other zones (Figure 5c). This pattern also applies to metabolically related compounds: compared to the basal zone and the apices, the middle zone contains more galactose, mannose, and glyceric acid (components of floridoside and digeneaside), but less glucose (monomer of floridean starch) (Figure 9). Such a carbohydrate profile suggests that the cells invest most of the assimilated carbon into the synthesis of structural polysaccharides, strengthening and thickening cell walls, as well as into a mobile fraction of storage compounds that could be transported to the sink zones of the thallus, such as apices or rhizoids.

Regarding secondary metabolites, relatively low levels of phenolic acids were detected in the mid-thallus of *Furcellaria* in both the spectrophotometric assay (Figure 4b) and GC-MS analysis (Figure 8). However, surprisingly, TPC values were similar throughout the thallus (Figure 4a). The simplest and most likely explanation for this discrepancy is the presence of some phenolic metabolites in the cells of the mid-thallus that fall outside the detection scope of our methods. These can be molecules that lack the catecholic moieties required for detection using the protocol of Pękal et al. [42] and others that may be too large or too labile to be reliably analyzed by GC-MS. According to the literature data, flavonoids such as morin, hesperetin, genistein, daidzein, etc., could be expected in gigartinalean algae [106,107]; further research is needed to clarify this issue.

The only group of phenolic acids specifically accumulating in the middle zone of the *Furcellaria* thallus includes the derivatives of 4-hydroxyphenylacetic acid, such as 3,4-dihydroxyphenylacetate and mono- and dihydroxymandelic acid (Figure 8). These compounds are regarded as characteristic intermediates of the catabolic route for aromatic amino acids [108]. Thus, in contrast to the apical zone, where active anabolic flux supports chemical defense, the middle zone appears to channel a portion of its phenylpropanoid metabolism towards degradative or side-chain remodeling pathways. Interestingly, 4-hydroxyphenylacetic and 4-hydroxymandelic acids were shown to be precursors in the biosynthesis of bromophenols in the Ceramiales alga, *Odonthalia dentata* [109]. Although, with few exceptions, bromophenol production is not typical of the Gigartinales [110], the occurrence of these compounds in *F. lumbricalis* raises intriguing questions regarding the evolution of phenolic metabolism in red algae.

4.3.3. Basal Zone of the Thallus

The basal zone of the *F. lumbricalis* thallus is the oldest part of the organism (Figure 1). Typically, the thallus in this zone is heavily pigmented, relatively thin, and rigid, compared to the middle zone. According to our data, certain biochemical characteristics of *Furcellaria* base share common features with either the mid-thallus or apices. The pigment content and the TPC (Figures 2–4), as well as relative amounts of predominant low-molecular-weight carbohydrates (floridoside, digeneaside) and fatty acids (Figures 7 and 9) in the basal zone are closer to the values in the mid-thallus than to the ones in the apices, while the content of floridean starch, glucose, free amino acids and some phenolic metabolites (Figures 5

and 7–9) is similar to that in the apices. This pattern is reflected in the results of discriminant analysis of metabolomic data, where the first component brings together samples taken from the mid-thallus and base, whereas the second component combines those of base and apices (Figure 6). Such a specific biochemical profile suggests considerable metabolic activity and functional specialization of the basal thallus zone of *F. lumbricalis*.

The difference in cell age between the basal and middle zones may be responsible for the reduced galactose content in combination with the relatively high level of galactonic acid in the base of *Furcellaria* (Figure 7). Such a profile may indicate biochemical breakdown or remodeling of cell wall galactans as part of the natural wall autolysis occurring during algal senescence [111]. This is consistent with the lower carrageenan content observed in this zone, compared to the mid-thallus (Figure 5b).

The relatively high content of floridean starch and low-molecular-weight carbohydrates (heterosides, glucose, fructose, sucrose), including the compounds combining the functions of storing organic carbon and maintaining stress resistance (mannitol, trehalose, glycerol), implies an active role of the basal zone in resource storage and distribution, as well as in stress tolerance. In the case of trehalose and mannitol, such an uneven intra-thallus distribution with a peak in the basal zone (Figure 9) may be one of the explanations for why data on the occurrence of these metabolites in red algae are so scarce and sometimes ambiguous [51,67,69,71]. Routinely, samples for comparative biochemical studies of macroalgae have been taken from the mid-thallus, a zone which, in *F. lumbricalis*, has two times lower content of trehalose and more than ten times lower content of mannitol, compared to the basal zone (Figure 9).

Another group of metabolites accumulating in the base of the *Furcellaria* thallus and conferring stress resistance includes phenolic compounds such as *p*-coumaric acid (one of the dominant phenolics found in *F. lumbricalis*) and 3-phenyllactic acid (Figures 7 and 8). Coumaric acid is known as a strong antioxidant [98], and 3-phenyllactic acid is a potent antimicrobial and antifungal compound [112]. One more phenolic metabolite having the highest content in the basal thallus zone is a derivative of 4-hydroxymandelic acid, 4-hydroxybenzyl alcohol, also known as gastrodigenin (Figure 8). To date, the physiological role of this compound remains unexplored; however, its spatial localization in *F. lumbricalis* is intriguingly similar to that in terrestrial plants: in the orchid *Gastrodia elata* (Angiosperm), this alcohol is synthesized and accumulated in rhizomes [113].

Interestingly, our results have some degree of similarity to the data obtained on brown algae. Our previous study on the biochemical composition of *Fucus vesiculosus* showed several common features in the metabolite profiles of the apices and stipe of this alga [28], the same as between the apices and base of *Furcellaria* (Figures 6 and 7). E.g., studies on both *Fucus* and *Sargassum* (Phaeophyceae) have reported elevated mannitol levels in the mature basal parts of the thalli compared to the younger tissues [28,114], a pattern that also matches our observations in *F. lumbricalis*. Thus, even such evolutionarily distant species appear to share similar patterns in the biochemical composition of different thallus zones, reflecting deep functional specialization of their cells.

5. Conclusions

This study provides the first comprehensive biochemical characterization of different thallus zones of *F. lumbricalis*, as well as the first description of the low-molecular-weight metabolite profile of this commercially valuable alga. Our untargeted GC-MS approach revealed that the metabolome of *Furcellaria* is dominated by diverse carbohydrates (heterosides, polyols) and phenolic compounds. In particular, various phenolic acids and their derivatives account for 27% of the total annotated metabolome.

The pronounced biochemical heterogeneity across the thallus zones of *F. lumbricalis* implies their distinct functional specialization. Based on our data, we hypothesize that apical meristematic cells primarily rely on respiration for energy supply and may be characterized by active nitrogen metabolism. Carbon flux in the apices seems directed toward floridean starch and low-molecular-weight carbohydrates (isofloridoside, glucose, fructose, myo-inositol) rather than toward cell wall constituents. Elevated levels of specific phenolic acids (protocatechuic, dihydroxyphenylpyruvic) suggest a high activity of the shikimate pathway, which could protect young tissues from fouling and oxidative stress. The mid-thallus may function as a donor zone for the apices and base, storing mobile heterosides (floridoside, digeneaside) and investing in cell wall thickening, resulting in relatively high carrageenan content. The phenolic acid profile of these cells suggests active catabolism of phenylpropanoids. The basal zone exhibits considerable metabolic activity, accumulating mono- and disaccharides, sugar alcohols, floridean starch, and lipid metabolites, consistent with its hypothesized dual role in resource storage and stress tolerance. Characteristic antioxidant and antimicrobial phenolic compounds, such as *p*-coumaric and 3-phenyllactic acids, provide additional resilience to this zone.

Taken together, these findings establish a metabolic framework for understanding functional compartmentalization in red macroalgae. Further research is needed to elucidate and confirm eventual regulatory and transport mechanisms maintaining the biochemical gradients, as well as possible source–sink relationships within the thallus. In addition, a number of yet unknown compounds revealed by GC-MS analysis and presumed to be of phenolic nature provide a basis for further research into the biochemistry of red algae to expand the list of biologically active metabolites derived from seaweed.

Supplementary Materials: The following supporting information can be downloaded at https://www.mdpi.com/article/10.3390/phycology6040105/s1, Table S1: Low-molecular-weight metabolites detected by GC-MS analysis in methanolic extracts of *Furcellaria lumbricalis*; Figure S1: Validation parameters for the PLS-DA model; Figure S2: Mass spectral interpretation of the unknown peak at RI1349.

Author Contributions: Conceptualization, E.T.; methodology, C.W., E.Z. and E.T.; validation, E.T. and C.W.; formal analysis, E.Z., N.Y., S.B., C.W. and E.T.; investigation, E.Z., N.Y., C.W. and E.T.; resources, E.T. and C.W.; data curation, E.T. and C.W.; writing—original draft preparation, E.Z.; writing—review and editing, E.T. and C.W.; visualization, E.Z. and E.T.; supervision, E.T. and C.W.; project administration, E.T.; funding acquisition, E.T. All authors have read and agreed to the published version of the manuscript.

Funding: This research was supported by the Russian Science Foundation, grant No. 25-24-00114, https://rscf.ru/en/project/25-24-00114/ (accessed on 8 August 2026).

Institutional Review Board Statement: Not applicable.

Data Availability Statement: The datasets generated and/or analyzed in this study are available from the corresponding author upon reasonable request.

Acknowledgments: We thank the Marine Biological Station "UNB Belomorskaya" of St. Petersburg State University for providing facilities for sampling and the mass spectrometry core facility at the Faculty of Chemistry at Leipzig University, MS-UL, for carrying out the GC-MS analyses. Philipp Ristau and Ramona Oehme (Faculty of Chemistry, Leipzig University) are acknowledged for additional instrumental analyses to support the identification work for β-amino acid RI1349 (Figure S2).

Conflicts of Interest: The authors declare no conflicts of interest. The funders had no role in the design of the study; in the collection, analyses, or interpretation of data; in the writing of the manuscript; or in the decision to publish the results.

Abbreviations

The following abbreviations are used in this manuscript:

DW	Dry Weight
FW	Fresh Weight
GC-MS	Gas Chromatography–Mass Spectrometry
PLS-DA	Partial Least Squares Discriminant Analysis
RI	Retention Index
RT	Retention Time
TCA	Tricarboxylic Acid
TPC	Total Phenolic Content

References

1. Cai, J.; Lovatelli, A.; Garrido Gamarro, E.; Geehan, J.; Lucente, D.; Mair, G.; Miao, W.; Reantaso, M.; Roubach, R.; Yuan, X.; et al. *Seaweeds and Microalgae: An Overview for Unlocking Their Potential in Global Aquaculture Development*; FAO Fisheries and Aquaculture Circular No. 1229; FAO: Rome, Italy, 2021. [CrossRef]
2. FAO. *The State of World Fisheries and Aquaculture 2024—Blue Transformation in Action*; FAO: Rome, Italy, 2024. [CrossRef]
3. Bird, C.J.; Saunders, G.W.; McLachlan, J. Biology of *Furcellaria lumbricalis* (Hudson) Lamouroux (Rhodophyta: Gigartinales), a commercial carrageenophyte. *J. Appl. Phycol.* **1991**, *3*, 61–82. [CrossRef]
4. Bučas, M.; Daunys, D.; Olenin, S. Recent distribution and stock assessment of the red alga *Furcellaria lumbricalis* on an exposed Baltic Sea coast: Combined use of field survey and modeling methods. *Oceanologia* **2009**, *51*, 341–359. [CrossRef]
5. Kersen, P.; Martin, G. Annual biomass loss of the loose-lying red algal community via macroalgal beach casts in the Väinameri area, NE Baltic Sea. *Proc. Est. Acad. Sci. Biol. Ecol.* **2007**, *56*, 278–289. [CrossRef]
6. Paoli, R.; Foiadelli, C.; Traversi, M.; Tomasoni, G.; Romagnoli, F. Economic feasibility of *Furcellaria lumbricalis* biorefinery designs: A life cycle cost approach. *SSRN* **2025**, 5153254. [CrossRef]
7. Paalme, T.; Kotta, J.; Kersen, P.; Martin, G.; Kukk, H.; Torn, K. Inter-annual variations in biomass of loose lying algae *Furcellaria–Coccotylus* community: The relative importance of local versus regional environmental factors in the West Estonian archipelago. *Aquat. Bot.* **2011**, *95*, 146–152. [CrossRef]
8. Weinberger, F.; Paalme, T.; Wikström, S.A. Seaweed resources of the Baltic Sea, Kattegat and German and Danish North Sea coasts. *Bot. Mar.* **2020**, *63*, 61–72. [CrossRef]
9. Korolev, A.; Fetter, M. Monitoring of macro algae and blue mussels stocks in the Eastern Baltic. In Proceedings of the USA-Baltic International Symposium, Klaipeda, Lithuania, 15–17 June 2004. [CrossRef]
10. McLachlan, J.; Greenwell, M.G.; Bird, C.J.; Holmsgaard, J.E. Standing stocks of seaweeds of commercial importance on the north shore of Prince Edward island, Canada. *Bot. Mar.* **1987**, *30*, 277–290. [CrossRef]
11. Shoshina, E.V.; Makarevich, P.R. *Morskaya Botanika: Uchebnoe Posobie Dlya Vuzov [Marine Botany: A Textbook for Universities]*, 3rd ed.; Lan: St. Petersburg, Russia, 2023.
12. Marangoni Júnior, L.; Vieira, R.P.; Jamróz, E.; Anjos, C.A.R. Furcellaran: An innovative biopolymer in the production of films and coatings. *Carbohydr. Polym.* **2021**, *252*, 117221. [CrossRef]
13. Saluri, M.; Kaljuvee, K.L.; Paalme, T.; Reile, I.; Tuvikene, R. Structural variability and rheological properties of furcellaran. *Food Hydrocoll.* **2021**, *111*, 106227. [CrossRef]
14. Tuvikene, R. Carrageenans. In *Handbook of Hydrocolloids*, 3rd ed.; Phillips, G.O., Williams, P.A., Eds.; Woodhead Publishing: Duxford, UK, 2021; pp. 767–804. [CrossRef]
15. Tuvikene, R.; Truus, K.; Robal, M.; Volobujeva, O.; Mellikov, E.; Pehk, T.; Kollist, A.; Kailas, T.; Vaher, M. The extraction, structure, and gelling properties of hybrid galactan from the red alga *Furcellaria lumbricalis* (Baltic Sea, Estonia). *J. Appl. Phycol.* **2010**, *22*, 51–63. [CrossRef]
16. Nowak, E.; Żak, J.; Janik, M.; Cholewa-Wójcik, A.; Juszczak, L.; Szuwarzyński, M.; Mazur, T.; Konieczna-Molenda, A.; Jamróz, E. Double-layer films based on furcellaran/chitosan complex—Structural and functional characteristics of packaging materials. *Int. J. Mol. Sci.* **2025**, *26*, 10049. [CrossRef]
17. Zubia, M.; Fabre, M.S.; Kerjean, V.; Deslandes, E. Antioxidant and cytotoxic activities of some red algae (Rhodophyta) from Brittany Coasts (France). *Bot. Mar.* **2009**, *52*, 268–277. [CrossRef]
18. Saluri, M.; Kaldmäe, M.; Rospu, M.; Sirkel, H.; Paalme, T.; Landreh, M.; Tuvikene, R. Spatial variation and structural characteristics of phycobiliproteins from the red algae *Furcellaria lumbricalis* and *Coccotylus truncatus*. *Algal Res.* **2020**, *52*, 102058. [CrossRef]
19. Kersen, P.; Paalme, T.; Pajusalu, L.; Martin, G. Biotechnological applications of the red alga *Furcellaria lumbricalis* and its cultivation potential in the Baltic Sea. *Bot. Mar.* **2017**, *60*, 207–218. [CrossRef]

20. Naseri, A.; Holdt, S.L.; Jacobsen, C. Biochemical and nutritional composition of industrial red seaweed used in carrageenan production. *J. Aquat. Food Prod. Technol.* **2019**, *28*, 967–973. [CrossRef]
21. Kulikova, Y.; Sukhikh, S.; Kalashnikova, O.; Chupakhin, E.; Ivanova, S.; Chubarenko, B.; Gorbunova, J.; Babich, O. Assessment of the resource potential of Baltic Sea macroalgae. *Appl. Sci.* **2022**, *12*, 3599. [CrossRef]
22. Kostamo, K.; Olsson, S.; Korpelainen, H. Search for stress-responsive genes in the red alga *Furcellaria lumbricalis* (Rhodophyta) by expressed sequence tag analysis. *J. Exp. Mar. Bio. Ecol.* **2011**, *404*, 21–25. [CrossRef]
23. Olsson, S.; Korpelainen, H. Single nucleotide polymorphisms found in the red alga *Furcellaria lumbricalis* (Gigartinales): New markers for population and conservation genetic analyses. *Aquat. Conserv. Mar. Freshw. Ecosyst.* **2013**, *23*, 460–467. [CrossRef]
24. Nørskov, N.P.; Bruhn, A.; Cole, A.; Nielsen, M.O. Targeted and untargeted metabolic profiling to discover bioactive compounds in seaweeds and hemp using gas and liquid chromatography-mass spectrometry. *Metabolites* **2021**, *11*, 259. [CrossRef]
25. Lyons, D.A.; Van Alstyne, K.L.; Scheibling, R.E. Anti-grazing activity and seasonal variation of dimethylsulfoniopropionate-associated compounds in the invasive alga *Codium fragile* ssp. *tomentosoides*. *Mar. Biol.* **2007**, *153*, 179–188. [CrossRef]
26. Hay, M.E.; Steinberg, P.D. The chemical ecology of plant-herbivore interactions in marine versus terrestrial communities. In *Herbivores: Their Interactions with Secondary Plant Metabolites*, 2nd ed.; Rosenthal, G.A., Berenbaum, M.R., Eds.; Academic Press: San Diego, CA, USA, 1992; Volume II, pp. 371–413.
27. Schmid, M.; Stengel, D.B. Intra-thallus differentiation of fatty acid and pigment profiles in some temperate Fucales and Laminariales. *J. Phycol.* **2015**, *51*, 25–36. [CrossRef]
28. Birkemeyer, C.; Osmolovskaya, N.; Kuchaeva, L.; Tarakhovskaya, E. Distribution of natural ingredients suggests a complex network of metabolic transport between source and sink tissues in the brown alga *Fucus vesiculosus*. *Planta* **2019**, *249*, 377–391. [CrossRef]
29. Connan, S.; Delisle, F.; Deslandes, E.; Ar Gall, E. Intra-thallus phlorotannin content and antioxidant activity in Phaeophyceae of temperate waters. *Bot. Mar.* **2006**, *49*, 39–46. [CrossRef]
30. Katz, S.; Dubinsky, Z.; Rothmann, C.; Malik, Z.; Friedlander, M. Single-cell pigmentation of *Porphyra linearis* analyzed by Fourier transform multi-pixel spectroscopy and image analysis. *J. Phycol.* **1997**, *33*, 425–432. [CrossRef]
31. Che, S.; Du, G.; Zhong, X.; Mo, Z.; Wang, Z.; Mao, Y. Quantification of photosynthetic pigments in *Neopyropia yezoensis* using hyperspectral imagery. *Plant Phenomics* **2023**, *5*, 0012. [CrossRef]
32. Craigie, J.S.; Wen, Z.C. Effects of temperature and tissue age on gel strength and composition of agar from *Gracilaria tikvahiae* (Rhodophyceae). *Can. J. Bot.* **1984**, *62*, 1665–1670. [CrossRef]
33. Lechat, H.; Amat, M.; Mazoyer, J.; Gallant, D.J.; Buléon, A.; Lahaye, M. Cell wall composition of the carrageenophyte *Kappaphycus alvarezii* (Gigartinales, Rhodophyta) partitioned by wet sieving. *J. Appl. Phycol.* **1997**, *9*, 565–572. [CrossRef]
34. Phillips, D.W.; Towers, G.H.N. Chemical ecology of red algal bromophenols. I. Temporal, interpopulational and within-thallus measurements of lanosol levels in *Rhodomela larix* (Turner) C. Agardh. *J. Exp. Mar. Bio. Ecol.* **1982**, *58*, 285–293. [CrossRef]
35. García-Jiménez, P.; García-Maroto, F.; Garrido-Cárdenas, J.A.; Ferrandiz, C.; Robaina, R.R. Differential expression of the ornithine decarboxylase gene during carposporogenesis in the thallus of the red seaweed *Grateloupia imbricata* (Halymeniaceae). *J. Plant Physiol.* **2009**, *166*, 1745–1754. [CrossRef]
36. Indergaard, M.; Knutsen, S.H. Seasonal differences in ash, carbon, fibre and nitrogen components of *Furcellaria lumbricalis* (Gigartinales, Rhodophyceae), Norway. *Bot. Mar.* **1990**, *33*, 327–334. [CrossRef]
37. Barwell, C.J. Distribution of histamine in the thallus of *Furcellaria lumbricalis*. *J. Appl. Phycol.* **1989**, *1*, 341–344. [CrossRef]
38. Lichtenthaler, H.K.; Buschmann, C. Chlorophylls and carotenoids: Measurement and characterization by UV-VIS spectroscopy. *Curr. Protoc. Food Anal. Chem.* **2001**, *1*, F4.3.1–F4.3.8. [CrossRef]
39. Ritchie, R.J. Consistent sets of spectrophotometric chlorophyll equations for acetone, methanol and ethanol solvents. *Photosynth. Res.* **2006**, *89*, 27–41. [CrossRef]
40. Lüder, U.H.; Wiencke, C.; Knoetzel, J. Acclimation of photosynthesis and pigments during and after six months of darkness in *Palmaria decipiens* (Rhodophyta): A study to simulate Antarctic winter sea ice cover. *J. Phycol.* **2002**, *38*, 904–913. [CrossRef]
41. Cicco, N.; Lanorte, M.T.; Paraggio, M.; Viggiano, M.; Lattanzio, V. A Reproducible, rapid and inexpensive Folin–Ciocalteu micro-method in determining phenolics of plant methanol extracts. *Microchem. J.* **2009**, *91*, 107–110. [CrossRef]
42. Pękal, A.; Pyrzynska, K. Evaluation of aluminium complexation reaction for flavonoid content assay. *Food Anal. Methods* **2014**, *7*, 1776–1782. [CrossRef]
43. Huijgen, W.J.J.; Cobussen-Pool, E.M.; van Egmond, B.F.; van Hal, J.W. Determination of carbohydrate composition of macroalgae. In *Protocols for Macroalgae Research*; CRC Press: Boca Raton, FL, USA, 2018; pp. 199–210. [CrossRef]
44. Hewitt, B.R. Spectrophotometric determination of total carbohydrate. *Nature* **1958**, *182*, 246–247. [CrossRef]
45. Yu, G.; Yang, B.; Ren, W.; Zhao, X.; Zhang, J.; Barrow, C. A Comparative analysis of four kinds of polysaccharides purified from *Furcellaria lumbricalis*. *J. Ocean Univ. China* **2007**, *6*, 16–20. [CrossRef]
46. Freile-Pelegrín, Y.; Azamar, J.A.; Robledo, D. Preliminary characterization of carrageenan from the red seaweed *Halymenia floresii*. *J. Aquat. Food Prod. Technol.* **2011**, *20*, 73–83. [CrossRef]

47. Hutschenreuther, A.; Kiontke, A.; Birkenmeier, G.; Birkemeyer, C. Comparison of extraction conditions and normalization approaches for cellular metabolomics of adherent growing cells with GC-MS. *Anal. Methods* **2012**, *4*, 1953–1963. [CrossRef]
48. Kováts, E. Gas-chromatographische Charakterisierung organischer Verbindungen. Teil 1: Retentionsindices aliphatischer Halogenide, Alkohole, Aldehyde und Ketone. *Helv. Chim. Acta* **1958**, *41*, 1915–1932. [CrossRef]
49. Kopka, J.; Schauer, N.; Krueger, S.; Birkemeyer, C.; Usadel, B.; Bergmüller, E.; Dörmann, P.; Weckwerth, W.; Gibon, Y.; Stitt, M.; et al. GMD@CSB.DB: The Golm Metabolome Database. *Bioinformatics* **2005**, *21*, 1635–1638. [CrossRef]
50. Tolpeznikaite, E.; Bartkevics, V.; Ruzauskas, M.; Pilkaityte, R.; Viskelis, P.; Urbonaviciene, D.; Zavistanaviciute, P.; Zokaityte, E.; Ruibys, R.; Bartkiene, E. Characterization of macro- and microalgae extracts bioactive compounds and micro- and macroelements transition from algae to extract. *Foods* **2021**, *10*, 2226. [CrossRef]
51. Yanshin, N.; Kushnareva, A.; Lemesheva, V.; Birkemeyer, C.; Tarakhovskaya, E. Chemical composition and potential practical application of 15 red algal species from the White Sea coast (the Arctic Ocean). *Molecules* **2021**, *26*, 2489. [CrossRef]
52. Ismail, M.M.; Osman, M.E.H. Seasonal fluctuation of photosynthetic pigments of most common red seaweeds species collected from Abu Qir, Alexandria, Egypt. *Rev. Biol. Mar. Oceanogr.* **2016**, *51*, 515–525. [CrossRef]
53. Suresh Kumar, K.; Kumari, S.; Singh, K.; Kushwaha, P. Influence of seasonal variation on chemical composition and nutritional profiles of macro- and microalgae. In *Recent Advances in Micro and Macroalgal Processing: Food and Health Perspectives*; John Wiley & Sons: Hoboken, NJ, USA, 2021; pp. 14–71. [CrossRef]
54. Saluri, M.; Kaldmäe, M.; Tuvikene, R. Extraction and quantification of phycobiliproteins from the red alga *Furcellaria lumbricalis*. *Algal Res.* **2019**, *37*, 115–123. [CrossRef]
55. Tuvikene, R.; Robal, M. *Valgulised Pigmendid Läänemere Punavetikast Furcellaria lumbricalis: Sisaldus ja Eraldamisvõimalused*; Tallinn University: Tallinn, Estonia, 2015; p. 36.
56. Parjikolaei, B.R.; Bruhn, A.; Eybye, K.L.; Larsen, M.M.; Rasmussen, M.B.; Christensen, K.V.; Fretté, X.C. Valuable biomolecules from nine North Atlantic red macroalgae: Amino acids, fatty acids, carotenoids, minerals and metals. *Nat. Resour.* **2016**, *7*, 157–183. [CrossRef]
57. Olsson, J.; Toth, G.B.; Albers, E. Biochemical composition of red, green and brown seaweeds on the Swedish West Coast. *J. Appl. Phycol.* **2020**, *32*, 3305–3317. [CrossRef]
58. Grasdalen, H.; Knutsen, S.H. Characterization of water-extractable polysaccharides from Norwegian *Furcellaria lumbricalis* (Huds.) Lamour. (Gigartinales, Rhodophyceae) by IR and NMR spectroscopy. *Bot. Mar.* **1987**, *30*, 497–506. [CrossRef]
59. Zhang, W.W.; Duan, X.J.; Huang, H.L.; Zhang, Y.; Wang, B.G. Evaluation of 28 marine algae from the Qingdao coast for antioxidative capacity and determination of antioxidant efficiency and total phenolic content of fractions and subfractions derived from *Symphyocladia latiuscula* (Rhodomelaceae). *J. Appl. Phycol.* **2007**, *19*, 97–108. [CrossRef]
60. Carpena, M.; Caleja, C.; Pereira, E.; Pereira, C.; Ćirić, A.; Soković, M.; Soria-Lopez, A.; Fraga-Corral, M.; Simal-Gandara, J.; Ferreira, I.C.F.R.; et al. Red seaweeds as a source of nutrients and bioactive compounds: Optimization of the extraction. *Chemosensors* **2021**, *9*, 132. [CrossRef]
61. Sabeena Farvin, K.H.; Jacobsen, C. Phenolic compounds and antioxidant activities of selected species of seaweeds from Danish coast. *Food Chem.* **2013**, *138*, 1670–1681. [CrossRef]
62. Wang, B.G.; Gloer, J.B.; Ji, N.Y.; Zhao, J.C. Halogenated organic molecules of Rhodomelaceae origin: Chemistry and biology. *Chem. Rev.* **2013**, *113*, 3632–3685. [CrossRef]
63. Barouti, A.; Vinh, L.B.; Herfindal, L.; Jordheim, M. Marine bromophenols from *Laminaria hyperborea*'s epiphytic biomass: Chemical profiling, cytotoxicity, and antioxidant activity. *Mar. Drugs* **2026**, *24*, 52. [CrossRef]
64. Paudel, P.; Wagle, A.; Seong, S.H.; Park, H.J.; Jung, H.A.; Choi, J.S. A new tyrosinase inhibitor from the red alga *Symphyocladia latiuscula* (Harvey) Yamada (Rhodomelaceae). *Mar. Drugs* **2019**, *17*, 295. [CrossRef]
65. Ishii, T.; Okino, T.; Suzuki, M.; Machiguchi, Y. Tichocarpols A and B, two novel phenylpropanoids with feeding-deterrent activity from the red alga *Tichocarpus crinitus*. *J. Nat. Prod.* **2004**, *67*, 1764–1766. [CrossRef]
66. Semmouri, I.; Paepen, R.; Janssen, C.R.; Asselman, J. Floridoside originating from red algae (Rhodophyta): Review on the occurrence, extraction and potential applications for human health and aquaculture. *Algal Res.* **2025**, *92*, 104376. [CrossRef]
67. Lindberg, B. Low-molecular carbohydrates in Algae. X. Investigation of *Furcellaria fastigiata*. *Acta Chem. Scand.* **1955**, *9*, 1093–1096. [CrossRef]
68. Kirst, G.O. Low MW carbohydrates and ions in Rhodophyceae: Quantitative measurement of floridoside and digeneaside. *Phytochemistry* **1980**, *19*, 1107–1110. [CrossRef]
69. Karsten, U.; Görs, S.; Eggert, A.; West, J.A. Trehalose, digeneaside, and floridoside in the Florideophyceae (Rhodophyta)—A reevaluation of its chemotaxonomic value. *Phycologia* **2007**, *46*, 143–150. [CrossRef]
70. Dickson, D.M.J.; Kirst, G.O. Osmotic adjustment in marine eukaryotic algae: The role of inorganic ions, quaternary ammonium, tertiary sulphonium and carbohydrate solutes: I. Diatoms and a rhodophyte. *New Phytol.* **1987**, *106*, 645–655. [CrossRef]
71. Kremer, B.P. Mannitol in the Rhodophyceae—A reappraisal. *Phytochemistry* **1976**, *15*, 1135–1138. [CrossRef]

72. Eggert, A.; Karsten, U. Low molecular weight carbohydrates in red algae—An ecophysiological and biochemical perspective. In *Red Algae in the Genomic Age*; Seckbach, J., Chapman, D.J., Eds.; Springer: Dordrecht, The Netherlands, 2010; pp. 443–456. [CrossRef]
73. Tonon, T.; Li, Y.; McQueen-Mason, S. Mannitol biosynthesis in algae: More widespread and diverse than previously thought. *New Phytol.* **2017**, *213*, 1573–1579. [CrossRef]
74. Hamid, S.S.; Wakayama, M.; Ichihara, K.; Sakurai, K.; Ashino, Y.; Kadowaki, R.; Soga, T.; Tomita, M. Metabolome profiling of various seaweed species discriminates between brown, red, and green algae. *Planta* **2019**, *249*, 1921–1947. [CrossRef]
75. Tarakhovskaya, E.; Gulk, E.; Zamyatkina, E. Non-proteinogenic amino acids from marine macroalgae: Diversity, functional roles, and biological activity. *Phycologia* **2025**, *64*, 366–388. [CrossRef]
76. Tamura, Y.; Takenaka, S.; Sugiyama, S.; Nakayama, R. Occurrence of anserine as an antioxidative dipeptide in a red alga, *Porphyra yezoensis*. *Biosci. Biotechnol. Biochem.* **1998**, *62*, 561–563. [CrossRef]
77. Fasakhodi, M.T.; Abed-Elmdoust, A.; Mirvaghefi, A.; Hosseini, S.V.; Tavabe, K.R. Changes of extracted bioactive compounds from brown algae (*Cystoseira indica*) after conversion to mill and tablet using a quantitative metabolomics approach. *Aquac. Int.* **2021**, *29*, 2793–2804. [CrossRef]
78. Fakhri, M.; Yoneda, K.; Maeda, Y.; Suzuki, I. Functional analysis of the carnosine synthase-like gene conserved in *Monoraphidium braunii*. *Algal Res.* **2024**, *78*, 103387. [CrossRef]
79. Koksharova, O.A.; Safronova, N.A. Non-proteinogenic amino acid β-N-methylamino-L-alanine (BMAA): Bioactivity and ecological significance. *Toxins* **2022**, *14*, 539. [CrossRef]
80. Blunden, G.; Smith, B.E.; Irons, M.W.; Yang, M.H.; Roch, O.G.; Patel, A.V. Betaines and tertiary sulphonium compounds from 62 species of marine algae. *Biochem. Syst. Ecol.* **1992**, *20*, 373–388. [CrossRef]
81. Turner, C.H.C.; Evans, L.V. Translocation of photoassimilated ^{14}C in the red alga *Polysiphonia lanosa*. *Br. Phycol. J.* **1978**, *13*, 51–55. [CrossRef]
82. Wetherbee, R. "Transfer connections": Specialized pathways for nutrient translocation in a red alga? *Science* **1979**, *204*, 858–859. [CrossRef]
83. Raven, J.A. Long-distance transport in non-vascular plants. *Plant Cell Environ.* **2003**, *26*, 73–85. [CrossRef]
84. Hartmann, T.; Eschrich, W. Stofftransport in Rotalgen. *Planta* **1969**, *85*, 303–312. [CrossRef]
85. Kim, G.H.; Nagasato, C.; Kwak, M.; Lee, J.W.; Young, C.; Klochkova, T.A.; Motomura, T. Intercellular transport across pit-connections in the filamentous red alga *Griffithsia monilis*. *Algae* **2022**, *37*, 75–84. [CrossRef]
86. Adamkiewicz-Chojnacka, B. Morphological and anatomical investigations of the species *Furcellaria fastigiata* (Huds.) Lam. from Puck Bay. *Oceanologia* **1983**, *16*, 133–147.
87. Dailer, M.L.; Smith, J.E.; Smith, C.M. Responses of bloom forming and non-bloom forming macroalgae to nutrient enrichment in Hawai'i, USA. *Harmful Algae* **2012**, *17*, 111–125. [CrossRef]
88. Parker, B.C. Translocation in *Macrocystis*. III. Composition of sieve tube exudate and identification of the major C^{14}-labeled products. *J. Phycol.* **1966**, *2*, 38–41. [CrossRef]
89. Diouris, M. Long-distance transport of ^{14}C-labelled assimilates in the Fucales: Nature of translocated substances in *Fucus serratus*. *Phycologia* **1989**, *28*, 504–511. [CrossRef]
90. Arnold, K.E.; Manley, S.L. Carbon allocation in *Macrocystis pyrifera* (Phaeophyta): Intrinsic variability in photosynthesis and respiration. *J. Phycol.* **1985**, *21*, 154–167. [CrossRef]
91. Bidel, L.P.R.; Renault, P.; Pagès, L.; Rivière, L.M. Mapping meristem respiration of *Prunus persica* (L.) Batsch seedlings: Potential respiration of the meristems, O2 diffusional constraints and combined effects on root growth. *J. Exp. Bot.* **2000**, *51*, 755–768. [CrossRef]
92. Chopin, T.; Hanisak, M.D.; Koehn, F.E. Effects of seawater phosphorus concentration on floridean starch content in *Agardhiella subulata* (C. Agardh) Kraft et Wynne (Rhodophyceae). *Bot. Mar.* **1991**, *34*, 369–373. [CrossRef]
93. Craigie, J.S.; McLachlan, J.; Tocher, R.D. Some neutral constituents of the Rhodophyceae with special reference to the occurrence of the floridosides. *Can. J. Bot.* **1968**, *46*, 605–611. [CrossRef]
94. Raven, J.A.; Johnston, A.M.; MacFarlane, J.J. Carbon Metabolism. In *Biology of the Red Algae*; Sheath, R.G., Cole, K.M., Eds.; Cambridge University Press: Cambridge, UK, 1990; pp. 171–202.
95. Karsten, U. Seaweed acclimation to salinity and desiccation stress. In *Seaweed Biology: Novel Insights into Ecophysiology, Ecology and Utilization*; Wiencke, C., Bischof, K., Eds.; Springer: Berlin/Heidelberg, Germany, 2012; pp. 87–107. [CrossRef]
96. Mao, J.; Zhu, Z.; Li, S.; Chen, H. Diel carbon buffering by floridoside enables source-sink resilience in the intertidal red alga *Pyropia haitanensis*. *J. Exp. Bot.* **2026**, *77*, 4634–4648. [CrossRef]
97. Chen, Q.; Zhu, B.; Sun, D.; Liu, W.; Sun, X.; Duan, S. The effect of protocatechuic acid on the phycosphere in harmful algal bloom species *Scrippsiella trochoidea*. *Aquat. Toxicol.* **2020**, *227*, 105591. [CrossRef]
98. Shanura Fernando, I.P.; Kim, M.; Son, K.T.; Jeong, Y.; Jeon, Y.J. Antioxidant activity of marine algal polyphenolic compounds: A mechanistic approach. *J. Med. Food* **2016**, *19*, 615–628. [CrossRef]

99. Khan, F.; Bamunuarachchi, N.I.; Tabassum, N.; Kim, Y.M. Caffeic acid and its derivatives: Antimicrobial drugs toward microbial pathogens. *J. Agric. Food Chem.* **2021**, *69*, 2979–3004. [CrossRef] [PubMed]
100. Mughal, A.; Jabeen, N.; Ashraf, K.; Sultan, K.; Farhan, M.; Hussain, M.I.; Deng, G.; Alsudays, I.M.; Saleh, M.A.; Tariq, S.; et al. Exploring the role of caffeic acid in mitigating abiotic stresses in plants: A review. *Plant Stress* **2024**, *12*, 100487. [CrossRef]
101. Petersen, M.; Abdullah, Y.; Benner, J.; Eberle, D.; Gehlen, K.; Hücherig, S.; Janiak, V.; Kim, K.H.; Sander, M.; Weitzel, C.; et al. Evolution of rosmarinic acid biosynthesis. *Phytochemistry* **2009**, *70*, 1663–1679. [CrossRef]
102. Hawas, U.W.; Husain, S.; El-Kassem, L.T.A. Biochemical composition and biological properties of some red and green algae from the Saudi Red Sea coast. *Thalass. Int. J. Mar. Sci.* **2025**, *41*, 104. [CrossRef]
103. Parthasarathy, A.; Savka, M.A.; Hudson, A.O. The synthesis and role of β-alanine in plants. *Front. Plant Sci.* **2019**, *10*, 921. [CrossRef]
104. Fries, L. Growth stimulation of axenic red algae by simple phenolic compounds. *J. Exp. Mar. Bio. Ecol.* **1974**, *15*, 1–9. [CrossRef]
105. Fries, L.; Iwasaki, H. p-Hydroxyphenylacetic acid and other phenolic compounds as growth stimulators of the red alga *Porphyra tenera*. *Plant Sci. Lett.* **1976**, *6*, 299–307. [CrossRef]
106. Yoshie-Stark, Y.; Hsieh, Y.-P.; Suzuki, T. Distribution of flavonoids and related compounds from seaweeds in Japan. *J. Tokyo Univ. Fish.* **2003**, *89*, 1–6.
107. Klejdus, B.; Lojková, L.; Plaza, M.; Šnóblová, M.; Štěrbová, D. Hyphenated technique for the extraction and determination of isoflavones in algae: Ultrasound-assisted supercritical fluid extraction followed by fast chromatography with tandem mass spectrometry. *J. Chromatogr. A* **2010**, *1217*, 7956–7965. [CrossRef]
108. Landymore, A.F. The Degradation of Phenylalanine, Tyrosine and Related Aromatic Compounds by a Marine Diatom and a Haptophycean Alga. Ph.D. Thesis, University of British Columbia, Vancouver, BC, Canada, 1976. [CrossRef]
109. Manley, S.L.; Chapman, D.J. Metabolism of L-tyrosine to 4-hydroxybenzaldehyde and 3-bromo-4-hydroxybenzaldehyde by chloroplast-containing fractions of *Odonthalia floccosa* (Esp.) Falk. *Plant Physiol.* **1979**, *64*, 1032–1038. [CrossRef]
110. Jacobtorweihen, J.; Spiegler, V. Phylogenetic distribution of bromophenols in marine algae and the generation of a comprehensive bromophenol database. *Phytochem. Rev.* **2022**, *22*, 505–542. [CrossRef]
111. Schlösser, U.G. Algal wall-degrading enzymes—Autolysines. In *Plant Carbohydrates II*; Tanner, W., Loewus, F.A., Eds.; Springer: Berlin/Heidelberg, Germany, 1981; pp. 333–351. [CrossRef]
112. Mu, W.; Yu, S.; Zhu, L.; Zhang, T.; Jiang, B. Recent research on 3-phenyllactic acid, a broad-spectrum antimicrobial compound. *Appl. Microbiol. Biotechnol.* **2012**, *95*, 1155–1163. [CrossRef]
113. Hayashi, J.; Sekine, T.; Deguchi, S.; Lin, Q.; Horie, S.; Tsuchiya, S.; Yano, S.; Watanabe, K.; Ikegami, F. Phenolic compounds from *Gastrodia* rhizome and relaxant effects of related compounds on isolated smooth muscle preparation. *Phytochemistry* **2002**, *59*, 513–519. [CrossRef]
114. Wong, S.Y.; Ang, P. Mannitol as a resource for the growth and reproduction of *Sargassum siliquastrum* (Mertens ex Turner) C. Agardh. *J. Appl. Phycol.* **2023**, *36*, 995–1008. [CrossRef]

Disclaimer/Publisher's Note: The statements, opinions and data contained in all publications are solely those of the individual author(s) and contributor(s) and not of MDPI and/or the editor(s). MDPI and/or the editor(s) disclaim responsibility for any injury to people or property resulting from any ideas, methods, instructions or products referred to in the content.